AFRL-RB-WP-TP-2011-3107

DYNAMICS AND CONTROL OF A BIOMIMETIC VEHICLE USING BIASED WINGBEAT FORCING FUNCTIONS: PART I - AERODYNAMIC MODEL (POSTPRINT)

David B. Doman, Michael W. Oppenheimer, and David O. Sigthorsson

Control Design and Analysis Branch
Control Sciences Division

JANUARY 2010

AIR FORCE RESEARCH LABORATORY
AIR VEHICLES DIRECTORATE
WRIGHT-PATTERSON AIR FORCE BASE, OH 45433-7542
AIR FORCE MATERIEL COMMAND
UNITED STATES AIR FORCE

REPORT DOCUMENTATION PAGE

Form Approved
OMB No. 0704-0188

1. REPORT DATE *(DD-MM-YY)*	2. REPORT TYPE	3. DATES COVERED *(From - To)*
January 2010	Conference Paper Postprint	13 August 2009 – 07 January 2010

4. TITLE AND SUBTITLE
DYNAMICS AND CONTROL OF A BIOMIMETIC VEHICLE USING BIASED WINGBEAT FORCING FUNCTIONS: PART I - AERODYNAMIC MODEL (POSTPRINT)

5a. CONTRACT NUMBER
In-house

5b. GRANT NUMBER

5c. PROGRAM ELEMENT NUMBER
62201F

6. AUTHOR(S)
David B. Doman, Michael W. Oppenheimer, and David O. Sigthorsson (AFRL/RBCA)

5d. PROJECT NUMBER
2401

5e. TASK NUMBER
N/A

5f. WORK UNIT NUMBER
Q12K

7. PERFORMING ORGANIZATION NAME(S) AND ADDRESS(ES)
Control Design and Analysis Branch (AFRL/RBCA)
Control Sciences Division
Air Force Research Laboratory, Air Vehicles Directorate
Wright-Patterson Air Force Base, OH 45433-7542
Air Force Materiel Command, United States Air Force

8. PERFORMING ORGANIZATION REPORT NUMBER
AFRL-RB-WP-TP-2011-3107

9. SPONSORING/MONITORING AGENCY NAME(S) AND ADDRESS(ES)
Air Force Research Laboratory
Air Vehicles Directorate
Wright-Patterson Air Force Base, OH 45433-7742
Air Force Materiel Command
United States Air Force

10. SPONSORING/MONITORING AGENCY ACRONYM(S)
AFRL/RBSD

11. SPONSORING/MONITORING AGENCY REPORT NUMBER(S)
AFRL-RB-WP-TP-2011-3107

12. DISTRIBUTION/AVAILABILITY STATEMENT
Approved for public release; distribution unlimited.

13. SUPPLEMENTARY NOTES
PAO Case Number: 88ABW-2009-5196; Clearance Date: 17 Dec 2009. Document contains color.

Conference paper published in the proceedings of the 48th AIAA Aerospace Sciences Meeting Including the New Horizons Forum and Aerospace Exposition held 4 - 7 January 2010 in Orlando, FL.

14. ABSTRACT
An aerodynamic model, for a minimally actuated flapping wing micro air vehicle (FWMAV), is derived from blade element theory. The vehicle considered in this work is similar to the Harvard RoboFly, except that it is equipped with independently actuated wings. A blade element-based approach is used to compute both instantaneous and cycle-averaged forces and moments for a specific type of wingbeat motion that enables nearly decoupled, multi-degree-of-freedom control of the aircraft. The wing positions are controlled using oscillators whose frequencies change once per wingbeat cycle. A technique is introduced, called Split-Cycle Constant-Period Frequency Modulation with Wing Bias, that provides a high level of control input decoupling for vehicles without active angle of attack control. This technique allows the frequencies of the upstroke and downstroke of each wing to differ such that non-zero cycle-averaged drag can be generated. Additionally, a wing bias term has been added to the wingbeat waveform and is utilized to provide pitching moment control. With this technique, it is possible to achieve five degree-of-freedom control using only two physical actuators. The present paper is concerned with the derivation of the instantaneous and cycle-averaged forces and moments for the Split- Cycle Constant-Period Frequency Modulation with Wing Bias technique. Implementation of the wing bias is discussed and modifications to the wingbeat forcing function, which are necessary to maintain a continuous wing position, are made.

15. SUBJECT TERMS
flapping wing micro air vehicles, MAV, flight control, minimal actuation, aerodynamic model, blade element theory

16. SECURITY CLASSIFICATION OF:			17. LIMITATION OF ABSTRACT:	18. NUMBER OF PAGES	19a. NAME OF RESPONSIBLE PERSON (Monitor)
a. REPORT	b. ABSTRACT	c. THIS PAGE			1Lt Zachary H. Goff
Unclassified	Unclassified	Unclassified	SAR	40	19b. TELEPHONE NUMBER *(Include Area Code)* N/A

48th AIAA Aerospace Sciences Meeting Including the New Horizons Forum and Aerospace Exposition
4 - 7 January 2010, Orlando, Florida

AIAA 2010-1023

Dynamics and Control of a Biomimetic Vehicle Using Biased Wingbeat Forcing Functions: Part I - Aerodynamic Model

Michael W. Oppenheimer *

David B. Doman †

David O. Sigthorsson ‡

An aerodynamic model, for a minimally actuated flapping wing micro air vehicle (FWMAV), is derived from blade element theory. The vehicle considered in this work is similar to the Harvard RoboFly, except that it is equipped with independently actuated wings. A blade element-based approach is used to compute both instantaneous and cycle-averaged forces and moments for a specific type of wingbeat motion that enables nearly decoupled, multi-degree-of-freedom control of the aircraft. The wing positions are controlled using oscillators whose frequencies change once per wingbeat cycle. A technique is introduced, called Split-Cycle Constant-Period Frequency Modulation with Wing Bias, that provides a high level of control input decoupling for vehicles without active angle of attack control. This technique allows the frequencies of the upstroke and downstroke of each wing to differ such that non-zero cycle-averaged drag can be generated. Additionally, a wing bias term has been added to the wingbeat waveform and is utilized to provide pitching moment control. With this technique, it is possible to achieve five degree-of-freedom control using only two physical actuators. The present paper is concerned with the derivation

*Senior Electronics Engineer, Control Design and Analysis Branch, 2210 Eighth Street, Ste 21, Air Force Research Laboratory, WPAFB, OH 45433-7531 Email Michael.Oppenheimer@wpafb.af.mil, Ph. (937) 255-8490, Fax (937) 656-4000, Associate Fellow AIAA

†Senior Aerospace Engineer, Control Design and Analysis Branch, 2210 Eighth Street, Ste 21, Air Force Research Laboratory, WPAFB, OH 45433-7531 Email David.Doman@wpafb.af.mil, Ph. (937) 255-8451, Fax (937) 656-4000, Associate Fellow AIAA

‡Electronics Engineer, Control Design and Analysis Branch, 2210 Eighth Street, Ste 21, Air Force Research Laboratory, WPAFB, OH 45433-7531 Email David.Sigthorsson@afmcx.net, Ph. (937) 255-9707, Fax (937) 656-4000, Member AIAA. This research was performed while this author held a National Research Council Research Associateship Award at the Air Force Research Laboratory.

of the instantaneous and cycle-averaged forces and moments for the Split-Cycle Constant-Period Frequency Modulation with Wing Bias technique. Implementation of the wing bias is discussed and modifications to the wing-beat forcing function, which are necessary to maintain a continuous wing position, are made.

I. Introduction

For years, researchers have been interested and intrigued by the flight of flapping wing insects. Some of the earliest research efforts on flapping wing vehicle flight took place in the 1950's and 1960's.[1–4] Osborne[1] used blade-element analysis to represent the forces on a flapping wing. Jensen[2] studied the flight of locusts while Vogel[3,4] analyzed the fruitfly Drosophila and calculated a lift coefficient for this insect. More recently, flapping wing micro air vehicles (MAVs) have received a great deal of interest from the research community due to their potential to achieve insect-like maneuverability.[5–11] The ability to mimic the flight behavior of insects could enable such a vehicle to perform missions which larger, fixed wing vehicles are unable to perform, such as intelligence, surveillance, and reconnaissance in urban environments and indoor locations. These potential capabilities have prompted continued research into flapping wing flight dynamics, control law development,[12,13] and fabrication.[7,8]

Biologists have been interested in insect flight for some time. Ellington[9,14–18] provided detailed analysis of hovering insect flight, including kinematics, lift and power requirements, and aerodynamic mechanisms. Other researchers have studied the flight of butterflies,[19] Diptera,[20] bumblebees,[10,11] and the hawkmoth Manduca Sexta.[21–23] The desire was to characterize and understand the mechanisms that enable insect flight.

The aerodynamics of flapping wing flight are complex.[9,14–18,24–27] Wing-wing interactions, wake capture, leading-edge vortices, wing rotation and acceleration are examples of some of the complex phenomena that occur. Dickinson[28] has studied the unsteady aerodynamics of model wings at low Reynolds numbers. Sane and Dickinson[6] have performed mineral oil experiments on a flapping wing and generated a quasi-steady aerodynamic model of the wing, while Sitaraman[29] developed a numerical model of the unsteady aerodynamics of flapping flight.

In this work, a simplified aerodynamic model, which does not take into account unsteady effects, is utilized for control law design. Deng,[30,31] Doman,[12,32] and Oppenheimer[13] have developed cycle-averaged control laws for flapping wing micro air vehicles. These control strategies used wing flip timing and mean angle of attack as control variables or included an additional control effector to adjust the center-of-gravity (CG) of the vehicle. The control strategy introduced by Deng[30] required 4 actuators. Oppenheimer[13] utilized split-cycle

constant period frequency modulation without wing bias to control a six degree-of-freedom (DOF) unsteady simulation model of a FWMAV using three actuators. Two actuators controlled wing position while the third controlled a bobweight. Here, the need for the bobweight actuator is eliminated by modifying the wingbeat profile to include a non-zero bias. The split-cycle constant period frequency technique[12,13] is still utilized, however, the wingbeat can be biased, which has the effect of providing control of the pitching moment. Due to the periodic nature of flapping wing motion, the forces produced by the wings are periodic functions of time. Thus, continuous control, of the forces and moments produced by the wings, is not an option and control variables should only be modified at the start of a cycle. Therefore, a cycle-averaged control law is developed and in this paper, the cycle-averaged forces and moments for a flapping wing MAV are computed. The vehicle used in this work is similar to the RoboFly[7] with a key difference being that the present vehicle has independently actuated wings.[12] Wood[7,8,33] has shown that liftoff can be achieved with these types of vehicles. The goal of this work is to provide a wingbeat forcing function and control law that can yield controlled six DOF flight of the vehicle using only two physical actuators.

A. Preliminary Assumptions

The purpose of this investigation is the development of a control strategy. Hence, an idealized model is desired, which allows one to study the dynamic behavior of the aircraft. This objective limits the fidelity of the aerodynamic and structural models that can be utilized. In light of the above objective, the following assumptions are made:

- There are no aerodynamic interactions between the left and right wings.
- There are no aerodynamic interactions between the wings and the fuselage.
- The passive wing rotation joint is on a limit when the wing angular velocity in the stroke plane is non-zero.
- The 2D sectional aerodynamic coefficients are known and constant throughout each stroke. Three dimensional and unsteady effects from leading edge vortex and wake phenomena are not present.
- The air mass surrounding the vehicle is quiescent.
- Aerodynamic forces and moments are the sole result of wing motion, i.e., only flight conditions in the neighborhood of hover are considered.
- The bandwidth of the piezoelectric actuators exceeds the wingbeat frequency.

A reduced-order model for control law design is developed. Ultimatley, the controller developed will be tested on a truth model that relaxes some of the assumptions made above and includes unsteady aerodynamic effects. Although the unsteady model is not developed here, it will be a focus of future research efforts.

II. Split-Cycle Constant-Period Frequency Modulation With Wing Bias

The wingbeat position command structure presented by Doman[12] was shown to be capable of producing horizontal and vertical forces as well as rolling and yawing moments. The inability of that control strategy to independently generate pitching moments led to the addition of a bobweight actuator. Here, a wing position bias is introduced that enables the cycle-averaged center-of-pressure of the beating wings to be moved such that cycle-averaged pitching moments can be manipulated without a bobweight. It will be shown that the new control strategy is capable of generating six independent forces and moments using only two physical actuators.

$$\begin{aligned} \phi_{u_{LW}}(t) &= A_{LW}\cos\left[\left(\omega_{LW}-\delta_{LW}\right)t\right]+\eta_{LW} \\ \phi_{d_{LW}}(t) &= A_{LW}\cos\left[\left(\omega_{LW}+\sigma_{LW}\right)t+\xi_{LW}\right]+\eta_{LW} \end{aligned} \tag{1}$$

and

$$\begin{aligned} \phi_{u_{RW}}(t) &= A_{RW}\cos\left[\left(\omega_{RW}-\delta_{RW}\right)t\right]+\eta_{RW} \\ \phi_{d_{RW}}(t) &= A_{RW}\cos\left[\left(\omega_{RW}+\sigma_{RW}\right)t+\xi_{RW}\right]+\eta_{RW} \end{aligned} \tag{2}$$

where $\phi_{u_{LW}}(t)$ is the wing position of the left wing on the upstroke, $\phi_{d_{LW}}(t)$ is the wing position of the left wing on the downstroke, $\phi_{u_{RW}}(t)$ is the wing position of the right wing on the upstroke, $\phi_{d_{RW}}(t)$ is the wing position of the right wing on the downstroke, η_{RW}, η_{LW} are the wing bias terms, and A_{RW}, A_{LW} are the wingbeat amplitudes. Practical implementation requires that the bias terms be delayed by one full wingbeat cycle for reasons that will become evident shortly. Changing the amplitude will have a similar effect as changing the fundamental wingbeat frequency because these variables change the wing velocities in the same way. Hence, either the amplitude or the wingbeat frequency can be a control variable. In this case, left and right wingbeat frequency will be used for control purposes, while the amplitude is maintained constant (with the exception of the necessary last quarter stroke amplitude change for wing position continuity with nonzero bias, which will be discussed shortly).

Figure 1 shows the effects, on the wingbeat forcing function, of changing the wing bias.

The wing bias is forced to be constant over each full cycle. Since $\eta_0 \neq \eta_1 \neq \eta_2$, discontinuities

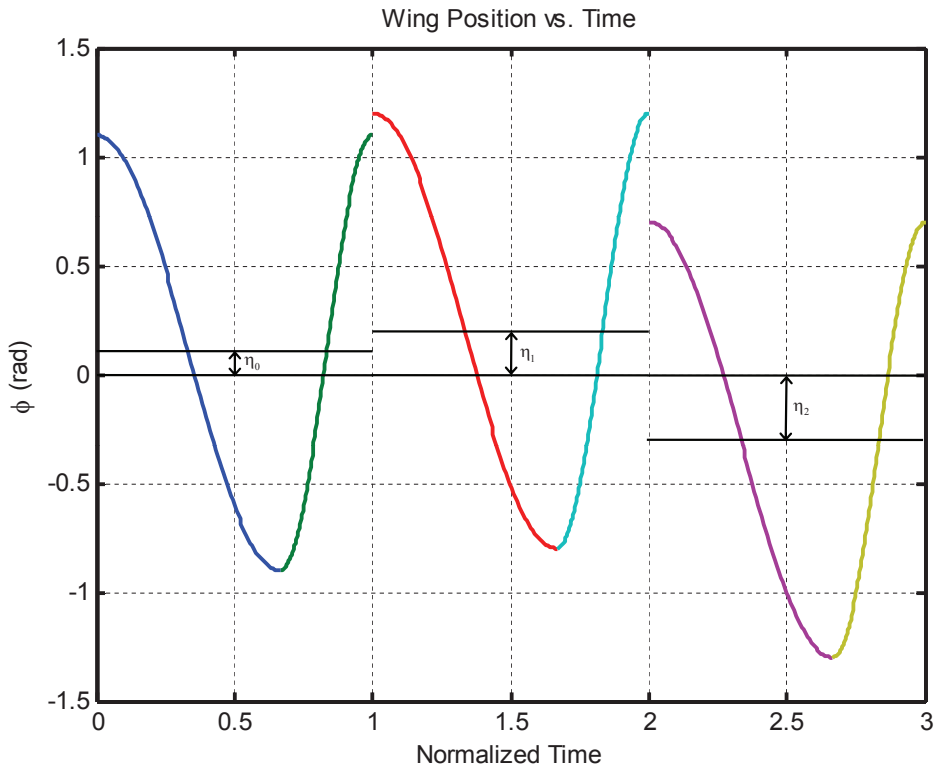

Figure 1. Wing Position With Variable η.

exist in the wing position. This is a situation that cannot physically exist. To overcome this issue, the second half of the downstroke is modified by the addition of a cosine wave. For the first half of the downstroke, the wing position forcing function is exactly as shown in Equations 1 and 2. For the second half of the downstroke, the wing position forcing functions are modified to the following form

$$\phi_{d_{LW}}(t) = A_{LW}\cos\left[\left(\omega_{LW}+\sigma_{LW}\right)t+\xi_{LW}\right]+\eta_{LW}+\Delta A_{LW}\cos\left[\left(\omega_{LW}+\sigma_{LW}\right)t+\xi_{LW}\right] \quad (3)$$

and

$$\phi_{d_{RW}}(t) = A_{RW}\cos\left[\left(\omega_{RW}+\sigma_{RW}\right)t+\xi_{RW}\right]+\eta_{RW}+\Delta A_{RW}\cos\left[\left(\omega_{RW}+\sigma_{RW}\right)t+\xi_{RW}\right] \quad (4)$$

The terms ΔA_{LW} and ΔA_{RW} are used to maintain a continuous wingbeat position forcing function. Figure 2 shows the results of adjusting the last half cycle of the downstroke. In this case, the wing position is continuous. Because frequency was chosen as a control variable instead of amplitude, this work utilizes constant amplitudes, i.e., $A_{LW} = A_{RW}$. Allowing the amplitude to vary between the up and downstrokes would force changes to the wingbeat

functions at the half and full cycle points of the wing motion to maintain a continuous wing position, whereas, changing the wing bias at the end of a full cycle only requires one modification to maintain a continuous wing position.

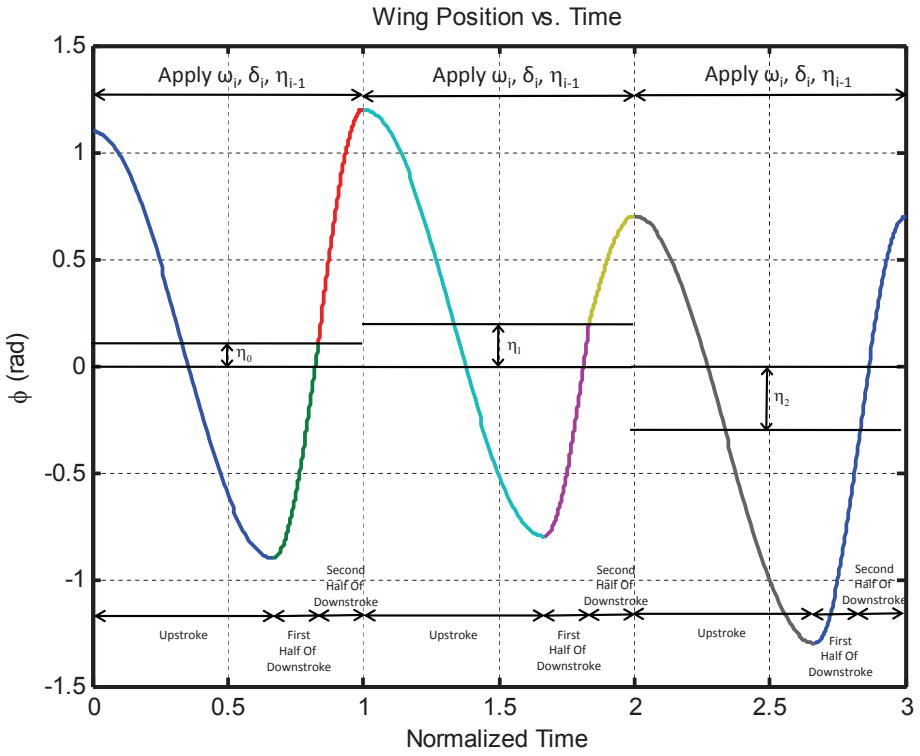

Figure 2. Wing Position With Variable η Altered to Maintain Continuity.

Figure 3 shows the points in the wingbeat cycle where $\omega_i, \delta_i, \eta_i, \Delta A_i$ are calculated and applied. Note that these variables are calculated at the beginning of the upstroke and that ΔA_i is applied for the last half of the downstroke to ensure wing position continuity. The bias term is delayed by one full wingbeat cycle and then is applied for the next complete wingbeat cycle. Thus, at the beginning of an upstroke, ω_i and δ_i are calculated and immediately applied for a complete cycle. Also, ΔA_i, A_i, and η_i are calculated with ΔA_i being applied for the last half of the current wingbeat downstroke and A_i and η_i being applied for the next full cycle.

In order to calculate the amplitude adjustment terms, consider the end of a complete wingbeat and, for brevity, consider only the left wing (right wing calculations are similar). Using Figure 3 and Equation 3, it can be seen that at the end of the first complete cycle, when $t = \frac{2\pi}{\omega}$, the modified downstroke wing position is

$$\phi_{d_{LW}}(t)|_{t=\frac{2\pi}{\omega}} = A_{LW_0} + \eta_{LW_0} + \Delta A_{LW_1} \tag{5}$$

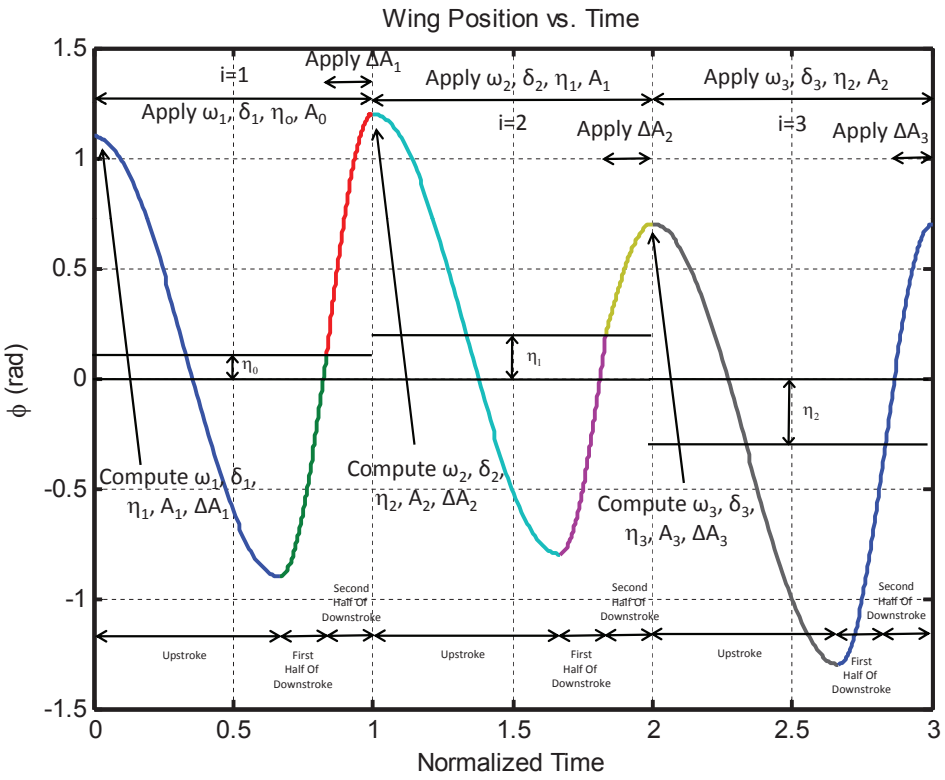

Figure 3. Points In Wingbeat Cycle Where Control Parameters Are Calculated And Applied.

while at the beginning of the second cycle upstroke, the wing position, Equation 1, is given by

$$\phi_{u_{LW}}(t)|_{t=\frac{2\pi}{\omega}} = A_{LW_1} + \eta_{LW_1} \tag{6}$$

Equating the expression in Equations 5 and 6 and solving for ΔA_{LW_1} yields

$$\Delta A_{LW_1} = A_{LW_1} + \eta_{LW_1} - (A_{LW_0} + \eta_{LW_0}) \tag{7}$$

In general, this expression becomes

$$\Delta A_i = A_i + \eta_i - (A_{i-1} + \eta_{i-1}) \tag{8}$$

Thus, in order to determine ΔA_i, the system needs information about the amplitude and bias during the next wingbeat cycle.

The forcing functions driving the positions of the wings are

$$\begin{aligned}
\phi_{u_{LW}}(t) &= A_{LW}\cos\left[\left(\omega_{LW}-\delta_{LW}\right)t\right]+\eta_{LW}\ \ \text{(upstroke)}\\
\phi_{d_{LW}}(t) &= A_{LW}\cos\left[\left(\omega_{LW}+\sigma_{LW}\right)t+\xi_{LW}\right]+\eta_{LW}\ \ \left(\text{first }\frac{1}{2}\text{ of downstroke}\right)\\
\phi_{d_{LW}}(t) &= \left(A_{LW}+\Delta A_{LW}\right)\cos\left[\left(\omega_{LW}+\sigma_{LW}\right)t+\xi_{LW}\right]+\eta_{LW}\ \ \left(\text{second }\frac{1}{2}\text{ of downstroke}\right)
\end{aligned} \tag{9}$$

and

$$\begin{aligned}
\phi_{u_{RW}}(t) &= A_{RW}\cos\left[\left(\omega_{RW}-\delta_{RW}\right)t\right]+\eta_{RW}\ \ \text{(upstroke)}\\
\phi_{d_{RW}}(t) &= A_{RW}\cos\left[\left(\omega_{RW}+\sigma_{RW}\right)t+\xi_{RW}\right]+\eta_{RW}\ \ \left(\text{first }\frac{1}{2}\text{ of downstroke}\right)\\
\phi_{d_{RW}}(t) &= \left(A_{RW}+\Delta A_{RW}\right)\cos\left[\left(\omega_{RW}+\sigma_{RW}\right)t+\xi_{RW}\right]+\eta_{RW}\ \ \left(\text{second }\frac{1}{2}\text{ of downstroke}\right)
\end{aligned} \tag{10}$$

It is important to point out that, in Equations 9 and 10, the time index subscripts on the variables have not been included. It should be understood that for wingbeat cycle i, the biases and amplitudes used are $\eta_{LW_{i-1}}, \eta_{RW_{i-1}}, A_{RW_{i-1}}, A_{LW_{i-1}}$ while the fundamental frequency ω_{RW}, ω_{LW}, split-cycle parameters δ_{RW}, δ_{LW}, and amplitude modification parameters $\Delta A_{RW}, \Delta A_{LW}$ are the current time values. These variables are produced by the cycle-averaged control law presented in Part II.[34] In other words, bias and amplitude are delayed by one complete wingbeat cycle prior to their use in generating the wingbeat forcing functions.

III. Instantaneous Blade Element Model of Flapping Wing Vehicle with Independently Actuated Wings

In this section, an aerodynamic model of the flapping wing vehicle is developed. One of the objectives of this work is to develop a model which yields insight into the controllability of this class of vehicles. In light of this objective, the aerodynamic model is void of any unsteady effects and is based solely on blade element theory. The use of computational fluid dynamics or finite element models would provide a higher fidelity model, however, these techniques would not allow designers to make vehicle modifications and rapidly asses their effects and have a tendency to mask the most pertinent factors in force and moment generation.

A. Instantaneous Aerodynamic Forces and Centers-of-Pressure in Wing Planform Frames

The aerodynamic forces are derived, using blade element theory, for triangular shaped wings that have two degrees of freedom, namely, angular displacement, $\phi(t)$, about the wing root in the stroke plane, and angular displacement of the planform about the passive rotation hinge joint, which is equivalent to wing angle-of-attack, α, in still air. The lift and drag due to the wings was previously calculated[12] and is summarized here.

The lift and drag can be expressed as the product of time invariant parameters and time varying functions

$$\begin{aligned} L &= k_L \dot{\phi}(t)^2 \\ D &= k_D \dot{\phi}(t)^2 \end{aligned} \tag{11}$$

where

$$\begin{aligned} k_L &\triangleq \frac{\rho}{2} C_L(\alpha) I_A \\ k_D &\triangleq \frac{\rho}{2} C_D(\alpha) I_A \end{aligned} \tag{12}$$

ρ is the atmospheric density, I_A is the area moment of inertia of the planform about the wing root and $C_L(\alpha), C_D(\alpha)$ are the lift and drag coefficients, which are computed using the following expression from Sane and Dickinson[5]

$$\begin{aligned} C_L(\alpha) &= 1.58 \sin(2.13\alpha - 7.2) + 0.225 \\ C_D(\alpha) &= -1.55 \cos(2.04\alpha - 9.82) + 1.92 \end{aligned} \tag{13}$$

The only variable that can be actively manipulated to control the instantaneous aerodynamic forces is the angular velocity of the wing, $\dot{\phi}(t)$. Differentiating Equations 9 and 10 yields

$$\begin{aligned} \dot{\phi}_{u_{LW}}(t) &= -A_{LW}(\omega_{LW} - \delta_{LW}) \sin[(\omega_{LW} - \delta_{LW})\, t] \ \text{(upstroke)} \\ \dot{\phi}_{d_{LW}}(t) &= -A_{LW}(\omega_{LW} + \sigma_{LW}) \sin[(\omega_{LW} + \sigma_{LW})\, t + \xi_{LW}] \ \left(\text{first } \frac{1}{2} \text{ of downstroke}\right) \\ \dot{\phi}_{d_{LW}}(t) &= -(A_{LW} + \Delta A_{LW})(\omega_{LW} + \sigma_{LW}) \\ &\quad * \sin[(\omega_{LW} + \sigma_{LW})\, t + \xi_{LW}] \ \left(\text{second } \frac{1}{2} \text{ of downstroke}\right) \end{aligned} \tag{14}$$

and

$$
\begin{aligned}
\dot{\phi}_{u_{RW}}(t) &= -A_{RW}\left(\omega_{RW}-\delta_{RW}\right)\sin\left[\left(\omega_{RW}-\delta_{RW}\right)t\right]\ \text{(upstroke)}\\
\dot{\phi}_{d_{RW}}(t) &= -A_{RW}\left(\omega_{RW}+\sigma_{RW}\right)\sin\left[\left(\omega_{RW}+\sigma_{RW}\right)t+\xi_{RW}\right]\ \left(\text{first }\frac{1}{2}\text{ of downstroke}\right)\\
\dot{\phi}_{d_{RW}}(t) &= -\left(A_{RW}+\Delta A_{RW}\right)\left(\omega_{RW}+\sigma_{RW}\right)\\
&\quad *\sin\left[\left(\omega_{RW}+\sigma_{RW}\right)t+\xi_{RW}\right]\ \left(\text{second }\frac{1}{2}\text{ of downstroke}\right)
\end{aligned}
\tag{15}
$$

The instantaneous lift and drag of the left and right wings on the upstrokes and downstrokes are obtained by substituting Equations 14 and 15 into Equation 11 to yield

$$
\begin{aligned}
L_{u_{LW}} &= k_L A_{LW}^2\left(\omega_{LW}-\delta_{LW}\right)^2\sin^2\left[\left(\omega_{LW}-\delta_{LW}\right)t\right]\ \text{(upstroke)}\\
L_{d_{LW}} &= k_L A_{LW}^2\left(\omega_{LW}+\sigma_{LW}\right)^2\sin^2\left[\left(\omega_{LW}+\sigma_{LW}\right)t+\xi_{LW}\right]\ \left(\text{first }\frac{1}{2}\text{ of downstroke}\right)\\
L_{d_{LW}} &= k_L\left(A_{LW}+\Delta A_{LW}\right)^2\left(\omega_{LW}+\sigma_{LW}\right)^2\\
&\quad *\sin^2\left[\left(\omega_{LW}+\sigma_{LW}\right)t+\xi_{LW}\right]\ \left(\text{second }\frac{1}{2}\text{ of downstroke}\right)\\
D_{u_{LW}} &= k_D A_{LW}^2\left(\omega_{LW}-\delta_{LW}\right)^2\sin^2\left[\left(\omega_{LW}-\delta_{LW}\right)t\right]\ \text{(upstroke)}\\
D_{d_{LW}} &= k_D A_{LW}^2\left(\omega_{LW}+\sigma_{LW}\right)^2\sin^2\left[\left(\omega_{LW}+\sigma_{LW}\right)t+\xi_{LW}\right]\ \left(\text{first }\frac{1}{2}\text{ of downstroke}\right)\\
D_{d_{LW}} &= k_D\left(A_{LW}+\Delta A_{LW}\right)^2\left(\omega_{LW}+\sigma_{LW}\right)^2\\
&\quad *\sin^2\left[\left(\omega_{LW}+\sigma_{LW}\right)t+\xi_{LW}\right]\ \left(\text{second }\frac{1}{2}\text{ of downstroke}\right)
\end{aligned}
\tag{16}
$$

$$
\begin{aligned}
L_{u_{RW}} &= k_L A_{RW}^2\left(\omega_{RW}-\delta_{RW}\right)^2\sin^2\left[\left(\omega_{RW}-\delta_{RW}\right)t\right]\ \text{(upstroke)}\\
L_{d_{RW}} &= k_L A_{RW}^2\left(\omega_{RW}+\sigma_{RW}\right)^2\sin^2\left[\left(\omega_{RW}+\sigma_{RW}\right)t+\xi_{RW}\right]\ \left(\text{first }\frac{1}{2}\text{ of downstroke}\right)\\
L_{d_{RW}} &= k_L\left(A_{RW}+\Delta A_{RW}\right)^2\left(\omega_{RW}+\sigma_{RW}\right)^2\\
&\quad *\sin^2\left[\left(\omega_{RW}+\sigma_{RW}\right)t+\xi_{RW}\right]\ \left(\text{second }\frac{1}{2}\text{ of downstroke}\right)\\
D_{u_{RW}} &= k_D A_{RW}^2\left(\omega_{RW}-\delta_{RW}\right)^2\sin^2\left[\left(\omega_{RW}-\delta_{RW}\right)t\right]\ \text{(upstroke)}\\
D_{d_{RW}} &= k_D A_{RW}^2\left(\omega_{RW}+\sigma_{RW}\right)^2\sin^2\left[\left(\omega_{RW}+\sigma_{RW}\right)t+\xi_{RW}\right]\ \left(\text{first }\frac{1}{2}\text{ of downstroke}\right)\\
D_{d_{RW}} &= k_D\left(A_{RW}+\Delta A_{RW}\right)^2\left(\omega_{RW}+\sigma_{RW}\right)^2\\
&\quad *\sin^2\left[\left(\omega_{RW}+\sigma_{RW}\right)t+\xi_{RW}\right]\ \left(\text{second }\frac{1}{2}\text{ of downstroke}\right)
\end{aligned}
\tag{17}
$$

With the relationships between the body, roots, spars, upstroke planform and downstroke

planform axis systems established by Doman, et. al.,[12] the instantaneous values of lift and drag on each wing may be transformed into the body-axis coordinate frame. If the air mass is quiescent, then the relative wind is parallel to the stroke plane, which is coincident with the x-y plane of the local spar frames. Therefore, the lift and drag forces are conveniently expressed in the spar coordinate frames, which can be transformed to the body frame using rotation matrices.[12] The aerodynamic forces, associated with each wing and stroke expressed in the body frame, are summarized in Table 1.

Force	Body Frame
RW Upstroke	$\mathbf{F}^B_{u_{RW}} = \begin{bmatrix} L_{u_{RW}} \\ -D_{u_{RW}} \sin\phi_{u_{RW}}(t) \\ D_{u_{RW}} \cos\phi_{u_{RW}}(t) \end{bmatrix}$
RW Downstroke	$\mathbf{F}^B_{d_{RW}} = \begin{bmatrix} L_{d_{RW}} \\ D_{d_{RW}} \sin\phi_{d_{RW}}(t) \\ -D_{d_{RW}} \cos\phi_{d_{RW}}(t) \end{bmatrix}$
LW Upstroke	$\mathbf{F}^B_{u_{LW}} = \begin{bmatrix} L_{u_{LW}} \\ D_{u_{LW}} \sin\phi_{u_{LW}}(t) \\ D_{u_{LW}} \cos\phi_{u_{LW}}(t) \end{bmatrix}$
LW Downstroke	$\mathbf{F}^B_{d_{LW}} = \begin{bmatrix} L_{d_{LW}} \\ -D_{d_{LW}} \sin\phi_{d_{LW}}(t) \\ -D_{d_{LW}} \cos\phi_{d_{LW}}(t) \end{bmatrix}$

Table 1. Aerodynamic forces expressed in local spar and body frames.

In Table 1, the subscripts denote which wing and stroke while the superscript defines the axis system in which the force vector is written. For example, the subscript u_{RW} denotes the right wing upstroke while d_{RW} denotes the right wing downstroke. The superscript B denotes the body frame.

The center-of-pressure of each wing is conveniently expressed in the local wing planform frame associated with each stroke. The centers-of-pressure[12] of each wing on the upstroke and downstroke are summarized in Table 2. In Table 2, $\Delta\mathbf{r}^B_R$ is the position vector from the center-of-gravity to the origin of the right wing coordinate system, $\Delta\mathbf{r}^B_L$ is the position vector from the center-of-gravity to the origin of the left wing coordinate system, and x^{WP}_{cp}, y^{WP}_{cp} define the location of the center-of-pressure in the local wing planform frame. These position vectors are explicitly expressed as

CP Location	Body Frame Expression
RW Upstroke	$\mathbf{r}_{\mathbf{cp}_{u_{RW}}}^{B} = \begin{bmatrix} x_{cp}^{WP}\sin\alpha + \Delta x_R^B \\ x_{cp}^{WP}\sin\phi_{u_{RW}}\cos\alpha + y_{cp}^{WP}\cos\phi_{u_{RW}} + \frac{w}{2} \\ -x_{cp}^{WP}\cos\phi_{u_{RW}}\cos\alpha + y_{cp}^{WP}\sin\phi_{u_{RW}} + \Delta z_R^B \end{bmatrix}$
RW Downstroke	$\mathbf{r}_{\mathbf{cp}_{d_{RW}}}^{B} = \begin{bmatrix} x_{cp}^{WP}\sin\alpha + \Delta x_R^B \\ -x_{cp}^{WP}\sin\phi_{d_{RW}}\cos\alpha + y_{cp}^{WP}\cos\phi_{d_{RW}} + \frac{w}{2} \\ x_{cp}^{WP}\cos\phi_{d_{RW}}\cos\alpha + y_{cp}^{WP}\sin\phi_{d_{RW}} + \Delta z_R^B \end{bmatrix}$
LW Upstroke	$\mathbf{r}_{\mathbf{cp}_{u_{LW}}}^{B} = \begin{bmatrix} x_{cp}^{WP}\sin\alpha + \Delta x_L^B \\ -x_{cp}^{WP}\sin\phi_{u_{LW}}\cos\alpha - y_{cp}^{WP}\cos\phi_{u_{LW}} - \frac{w}{2} \\ -x_{cp}^{WP}\cos\phi_{u_{LW}}\cos\alpha + y_{cp}^{WP}\sin\phi_{u_{LW}} + \Delta z_L^B \end{bmatrix}$
LW Downstroke	$\mathbf{r}_{\mathbf{cp}_{d_{LW}}}^{B} = \begin{bmatrix} x_{cp}^{WP}\sin\alpha + \Delta x_L^B \\ x_{cp}^{WP}\sin\phi_{d_{LW}}\cos\alpha - y_{cp}^{WP}\cos\phi_{d_{LW}} - \frac{w}{2} \\ x_{cp}^{WP}\cos\phi_{d_{LW}}\cos\alpha + y_{cp}^{WP}\sin\phi_{d_{LW}} + \Delta z_L^B \end{bmatrix}$

Table 2. Centers-of-pressure expressed in body frame.

$$\Delta\mathbf{r}_R^B = \begin{bmatrix} \Delta x_R^B & \frac{w}{2} & \Delta z_R^B \end{bmatrix} \quad \Delta\mathbf{r}_L^B = \begin{bmatrix} \Delta x_L^B & -\frac{w}{2} & \Delta z_L^B \end{bmatrix} \tag{18}$$

where w is the width of the vehicle.

B. Aerodynamic Moments in Body Frame

The expressions for the aerodynamic moments associated with each wing and stroke are given by[12]

$$\begin{aligned} \mathbf{M}_{u_{RW}}^B &= \mathbf{r}_{\mathbf{cp}_{u_{RW}}}^{B} \times \mathbf{F}_{u_{RW}}^B \\ \mathbf{M}_{d_{RW}}^B &= \mathbf{r}_{\mathbf{cp}_{d_{RW}}}^{B} \times \mathbf{F}_{d_{RW}}^B \\ \mathbf{M}_{u_{LW}}^B &= \mathbf{r}_{\mathbf{cp}_{u_{LW}}}^{B} \times \mathbf{F}_{u_{LW}}^B \\ \mathbf{M}_{d_{LW}}^B &= \mathbf{r}_{\mathbf{cp}_{d_{LW}}}^{B} \times \mathbf{F}_{d_{LW}}^B \end{aligned} \tag{19}$$

Carrying out the cross product operations and substituting the values from Tables 2 and 1 into the expressions in Equation 19 yields[12]

$$\mathbf{M}^B_{u_{RW}} = \begin{bmatrix} D_{u_{RW}} \left[y^{WP}_{cp} + \frac{w}{2} \cos\phi_{u_{RW}} + \Delta z^B_R \sin\phi_{u_{RW}} \right] \\ \left\{ L_{u_{RW}} \left[y^{WP}_{cp} \sin\phi_{u_{RW}} + \Delta z^B_R \right] - D_{u_{RW}} \Delta x^B_R \cos\phi_{u_{RW}} - \dots \right. \\ \left. \left[L_{u_{RW}} \cos\alpha + D_{u_{RW}} \sin\alpha \right] x^{WP}_{cp} \cos\phi_{u_{RW}} \right\} \\ \left\{ -D_{u_{RW}} \Delta x^B_R \sin\phi_{u_{RW}} - L_{u_{RW}} \left[\frac{w}{2} + y^{WP}_{cp} \cos\phi_{u_{RW}} \right] - \dots \right. \\ \left. \left[L_{u_{RW}} \cos\alpha + D_{u_{RW}} \sin\alpha \right] x^{WP}_{cp} \sin\phi_{u_{RW}} \right\} \end{bmatrix} \tag{20}$$

$$\mathbf{M}^B_{d_{RW}} = \begin{bmatrix} -D_{d_{RW}} \left[y^{WP}_{cp} + \frac{w}{2} \cos\phi_{d_{RW}} + \Delta z^B_R \sin\phi_{d_{RW}} \right] \\ \left\{ L_{d_{RW}} \left[y^{WP}_{cp} \sin\phi_{d_{RW}} + \Delta z^B_R \right] + D_{d_{RW}} \Delta x^B_R \cos\phi_{d_{RW}} + \dots \right. \\ \left. \left[L_{d_{RW}} \cos\alpha + D_{d_{RW}} \sin\alpha \right] x^{WP}_{cp} \cos\phi_{d_{RW}} \right\} \\ \left\{ D_{d_{RW}} \Delta x^B_R \sin\phi_{d_{RW}} - L_{d_{RW}} \left[\frac{w}{2} + y^{WP}_{cp} \cos\phi_{d_{RW}} \right] + \dots \right. \\ \left. \left[L_{d_{RW}} \cos\alpha + D_{d_{RW}} \sin\alpha \right] x^{WP}_{cp} \sin\phi_{d_{RW}} \right\} \end{bmatrix} \tag{21}$$

$$\mathbf{M}^B_{u_{LW}} = \begin{bmatrix} D_{u_{LW}} \left[-y^{WP}_{cp} - \frac{w}{2} \cos\phi_{u_{LW}} - \Delta z^B_L \sin\phi_{u_{LW}} \right] \\ \left\{ L_{u_{LW}} \left[y^{WP}_{cp} \sin\phi_{u_{LW}} + \Delta z^B_L \right] - D_{u_{LW}} \Delta x^B_L \cos\phi_{u_{LW}} - \dots \right. \\ \left. \left[L_{u_{LW}} \cos\alpha + D_{u_{LW}} \sin\alpha \right] x^{WP}_{cp} \cos\phi_{u_{LW}} \right\} \\ \left\{ D_{u_{LW}} \Delta x^B_L \sin\phi_{u_{LW}} + L_{u_{LW}} \left[\frac{w}{2} + y^{WP}_{cp} \cos\phi_{u_{LW}} \right] + \dots \right. \\ \left. \left[L_{u_{LW}} \cos\alpha + D_{u_{LW}} \sin\alpha \right] x^{WP}_{cp} \sin\phi_{u_{LW}} \right\} \end{bmatrix} \tag{22}$$

$$\mathbf{M}^B_{d_{LW}} = \begin{bmatrix} D_{d_{LW}} \left[y^{WP}_{cp} + \frac{w}{2} \cos\phi_{d_{LW}} + \Delta z^B_L \sin\phi_{d_{LW}} \right] \\ \left\{ L_{d_{LW}} \left[y^{WP}_{cp} \sin\phi_{d_{LW}} + \Delta z^B_L \right] + D_{d_{LW}} \Delta x^B_L \cos\phi_{d_{LW}} + \dots \right. \\ \left. \left[L_{d_{LW}} \cos\alpha + D_{d_{LW}} \sin\alpha \right] x^{WP}_{cp} \cos\phi_{d_{LW}} \right\} \\ \left\{ -D_{d_{LW}} \Delta x^B_L \sin\phi_{d_{LW}} + L_{d_{LW}} \left[\frac{w}{2} + y^{WP}_{cp} \cos\phi_{d_{LW}} \right] - \dots \right. \\ \left. \left[L_{d_{LW}} \cos\alpha + D_{d_{LW}} \sin\alpha \right] x^{WP}_{cp} \sin\phi_{d_{LW}} \right\} \end{bmatrix} \tag{23}$$

Equations 20-23 provide the expressions for the instantaneous aerodynamic moments generated by each wing at any point in a wingbeat cycle in the body-axis coordinate frame.

In this work, the relationships between the cycle-averaged forces and moments and the wing kinematic parameters that can be manipulated for control are derived. These parameters are ω_{LW}, ω_{RW}, δ_{LW}, δ_{RW}, η_{LW}, and η_{RW}, which are the fundamental frequency, split-cycle parameters, and wing biases for the left and right wings, respectively, are derived. Feedback control laws based on cycle-averaged forces and moments will allow a vehicle to track desired angular and spatial positions in a mean sense; however, because of the true periodic nature of the aerodynamic forces, the vehicle will exhibit limit cycle behavior in a neighborhood about the mean position.

IV. Definite Integrals for Computation of Cycle-Averaged Aerodynamic Forces and Moments

In this section, expressions for the compute cycle-averaged forces and moments are derived. Since the introduction of the split-cycle parameter changes the frequency of the cosine wave when $(\omega - \delta)t = \pi$ in each cycle and because the downstroke is split into two parts, it is convenient to split the integrals, used to evaluate the cycle-averaged forces and moments, as follows

$$\overline{G} = \frac{\omega}{2\pi}\left[\int_0^{\frac{\pi}{\omega-\delta}} G(\phi_u(t))dt + \int_{\frac{\pi}{\omega-\delta}}^{\frac{\pi(3\omega-2\delta)}{2\omega(\omega-\delta)}} G(\phi_d(t))dt + \int_{\frac{\pi(3\omega-2\delta)}{2\omega(\omega-\delta)}}^{\frac{2\pi}{\omega}} G(\phi_d(t))dt\right] \tag{24}$$

where the downstroke is split into first-half and second-half parts. Note that G in Equation 24 is a generalized force that represents either a force or moment.

In order to calculate the cycle-averaged forces and moments, it will be necessary to evaluate numerous integrals. Many have no indefinite integral solutions. For example, many of the integrands will be of the form $\cos(\cos\omega t)$ or $\sin(\cos\omega t)$. Fortunately, definite integrals involving such functions exist over the intervals of interest for the present problem and can be derived from results presented in Gradshteyn & Ryzhik.[35] The solution of many of these definite integrals involve a Bessel function of the first kind, $J_1(\cdot)$, as well as a Struve function, $H_1(\cdot)$.[35] For convenience, the solutions to the definite integrals that are required to compute the cycle-averaged forces and moments are provided.

For the upstroke, there are three integrals of interest. The first is

$$I_1 \triangleq \int_0^{\frac{\pi}{\omega-\delta}} \sin^2\left[(\omega-\delta)t\right] dt = \frac{\pi}{2(\omega-\delta)} \tag{25}$$

The second integral used during the upstroke is

$$I_2 \triangleq \int_0^{\frac{\pi}{\omega-\delta}} \sin^2\left[(\omega-\delta)t\right] \sin\left(A\cos\left[(\omega-\delta)t\right] + \eta\right) dt \tag{26}$$

Using the following identity,

$$\sin(\beta+\eta) = \sin\beta\cos\eta + \cos\beta\sin\eta \tag{27}$$

Equation 26 can be rewritten as

$$\begin{aligned} I_2 \triangleq & \int_0^{\frac{\pi}{\omega-\delta}} \sin^2\left[(\omega-\delta)t\right] \sin\left(A\cos\left[(\omega-\delta)t\right]\right)\cos\eta dt \\ & + \int_0^{\frac{\pi}{\omega-\delta}} \sin^2\left[(\omega-\delta)t\right] \cos\left(A\cos\left[(\omega-\delta)t\right]\right)\sin\eta dt = I_{21}+I_{22} \end{aligned} \tag{28}$$

Evaluating the integrals yields

$$I_{21} = 0 \quad I_{22} = \tfrac{\pi}{A(\omega-\delta)} J_1(A)\sin\eta \tag{29}$$

where $J_1(A)$ is a bessel function of the first kind. The last upstroke integral necessary to compute cycle-averaged forces and moments is

$$I_3 \triangleq \int_0^{\frac{\pi}{\omega-\delta}} \sin^2\left[(\omega-\delta)t\right] \cos\left(A\cos\left[(\omega-\delta)t\right]+\eta\right) dt \tag{30}$$

Using the following identity,

$$\cos\left(\beta+\eta\right) = \cos\beta\cos\eta - \sin\beta\sin\eta \tag{31}$$

Equation 30 can be rewritten as

$$\begin{aligned} I_3 \triangleq & \int_0^{\frac{\pi}{\omega-\delta}} \sin^2\left[(\omega-\delta)t\right] \cos\left(A\cos\left[(\omega-\delta)t\right]\right)\cos\eta dt \\ & - \int_0^{\frac{\pi}{\omega-\delta}} \sin^2\left[(\omega-\delta)t\right] \sin\left(A\cos\left[(\omega-\delta)t\right]\right)\sin\eta dt = I_{31}+I_{32} \end{aligned} \tag{32}$$

Evaluating the integrals yields

$$I_{31} = \tfrac{\pi}{A(\omega-\delta)} J_1(A)\cos\eta \quad I_{32} = 0 \tag{33}$$

Since the second half of the downstroke is modified to ensure wing position continuity, integrals over the downstroke become more complicated than those over the upstroke. In fact, the integrals are split into two parts. The first downstroke integral is

$$\begin{aligned} I_4 \triangleq & \int_{\frac{\pi}{\omega-\delta}}^{\frac{\pi(3\omega-2\delta)}{2\omega(\omega-\delta)}} \sin^2\left[(\omega+\sigma)t+\xi\right] dt + \int_{\frac{\pi(3\omega-2\delta)}{2\omega(\omega-\delta)}}^{\frac{2\pi}{\omega}} \sin^2\left[(\omega+\sigma)t+\xi\right] dt \\ = & \frac{\pi}{4(\omega+\sigma)} + \frac{\pi}{4(\omega+\sigma)} = I_{41}+I_{42} \end{aligned} \tag{34}$$

The fifth integral is

$$\begin{aligned} I_5 \triangleq & \int_{\frac{\pi}{\omega-\delta}}^{\frac{\pi(3\omega-2\delta)}{2\omega(\omega-\delta)}} \sin^2\left[(\omega+\sigma)t+\xi\right] \sin\left(A\cos\left[(\omega+\sigma)t+\xi\right]+\eta\right) dt \\ & + \int_{\frac{\pi(3\omega-2\delta)}{2\omega(\omega-\delta)}}^{\frac{2\pi}{\omega}} \sin^2\left[(\omega+\sigma)t+\xi\right] \sin\left(\{A+\Delta A\}\cos\left[(\omega+\sigma)t+\xi\right]+\eta\right) dt \end{aligned} \tag{35}$$

Using the identity in Equation 27, I_5 can be written as

$$\begin{aligned} I_5 \triangleq & \int_{\frac{\pi}{\omega-\delta}}^{\frac{\pi(3\omega-2\delta)}{2\omega(\omega-\delta)}} \sin^2\left[(\omega+\sigma)t+\xi\right] \sin\left(A\cos\left[(\omega+\sigma)t+\xi\right]\right)\cos\eta dt \\ & + \int_{\frac{\pi}{\omega-\delta}}^{\frac{\pi(3\omega-2\delta)}{2\omega(\omega-\delta)}} \sin^2\left[(\omega+\sigma)t+\xi\right] \cos\left(A\cos\left[(\omega+\sigma)t+\xi\right]\right)\sin\eta dt \\ & + \int_{\frac{\pi(3\omega-2\delta)}{2\omega(\omega-\delta)}}^{\frac{2\pi}{\omega}} \sin^2\left[(\omega+\sigma)t+\xi\right] \sin\left(\{A+\Delta A\}\cos\left[(\omega+\sigma)t+\xi\right]\right)\cos\eta dt \\ & + \int_{\frac{\pi(3\omega-2\delta)}{2\omega(\omega-\delta)}}^{\frac{2\pi}{\omega}} \sin^2\left[(\omega+\sigma)t+\xi\right] \cos\left(\{A+\Delta A\}\cos\left[(\omega+\sigma)t+\xi\right]\right)\sin\eta dt \\ & = I_{51}+I_{52}+I_{53}+I_{54} \end{aligned} \tag{36}$$

where

$$\begin{aligned} I_{51} &= \tfrac{-\pi}{2A(\omega+\sigma)} H_1(A)\cos\eta \\ I_{52} &= \tfrac{\pi}{2A(\omega+\sigma)} J_1(A)\sin\eta \\ I_{53} &= \tfrac{\pi}{2\{A+\Delta A\}(\omega+\sigma)} H_1(A+\Delta A)\cos\eta \\ I_{54} &= \tfrac{\pi}{2\{A+\Delta A\}(\omega+\sigma)} J_1(A+\Delta A)\sin\eta \end{aligned} \tag{37}$$

and $H_1(\cdot)$ is a Struve function. The last integral of interest is

$$\begin{aligned} I_6 \triangleq & \int_{\frac{\pi}{\omega-\delta}}^{\frac{\pi(3\omega-2\delta)}{2\omega(\omega-\delta)}} \sin^2\left[(\omega+\sigma)t+\xi\right] \cos\left(A\cos\left[(\omega+\sigma)t+\xi\right]+\eta\right) dt \\ & + \int_{\frac{\pi(3\omega-2\delta)}{2\omega(\omega-\delta)}}^{\frac{2\pi}{\omega}} \sin^2\left[(\omega+\sigma)t+\xi\right] \cos\left(\{A+\Delta A\}\cos\left[(\omega+\sigma)t+\xi\right]+\eta\right) dt \end{aligned} \tag{38}$$

Using the identity in Equation 31, Equation 38 can be rewritten as

$$\begin{aligned}
I_6 \triangleq & \int_{\frac{\pi}{\omega-\delta}}^{\frac{\pi(3\omega-2\delta)}{2\omega(\omega-\delta)}} \sin^2\left[(\omega+\sigma)t+\xi\right]\cos\left(A\cos\left[(\omega+\sigma)t+\xi\right]\right)\cos\eta dt \\
& - \int_{\frac{\pi}{\omega-\delta}}^{\frac{\pi(3\omega-2\delta)}{2\omega(\omega-\delta)}} \sin^2\left[(\omega+\sigma)t+\xi\right]\sin\left(A\cos\left[(\omega+\sigma)t+\xi\right]\right)\sin\eta dt \\
& + \int_{\frac{\pi(3\omega-2\delta)}{2\omega(\omega-\delta)}}^{\frac{2\pi}{\omega}} \sin^2\left[(\omega+\sigma)t+\xi\right]\cos\left(\{A+\Delta A\}\cos\left[(\omega+\sigma)t+\xi\right]\right)\cos\eta dt \\
& - \int_{\frac{\pi(3\omega-2\delta)}{2\omega(\omega-\delta)}}^{\frac{2\pi}{\omega}} \sin^2\left[(\omega+\sigma)t+\xi\right]\sin\left(\{A+\Delta A\}\cos\left[(\omega+\sigma)t+\xi\right]\right)\sin\eta dt \\
& = I_{61}+I_{62}+I_{63}+I_{64}
\end{aligned} \tag{39}$$

where

$$\begin{aligned}
I_{61} &= \tfrac{\pi}{2A(\omega+\sigma)} J_1(A)\cos\eta \\
I_{62} &= \tfrac{\pi}{2A(\omega+\sigma)} H_1(A)\sin\eta \\
I_{63} &= \tfrac{\pi}{2\{A+\Delta A\}(\omega+\sigma)} J_1(A+\Delta A)\cos\eta \\
I_{64} &= \tfrac{-\pi}{2\{A+\Delta A\}(\omega+\sigma)} H_1(A+\Delta A)\sin\eta
\end{aligned} \tag{40}$$

V. Cycle-Averaged Forces and Moments

The cycle-averaged aerodynamic forces and moments in the body frame will now be calculated. The cycle-averaged forces and moments will eventually form the basis for the computation of sensitivities to changes in control parameters. These cycle-averaged sensitivities form the control effectiveness matrix, which is used to compute the wingbeat kinematic parameters. These kinematic parameters produce the cycle-averaged forces and moments that are commanded by a feedback control law that regulates the mean motion of the vehicle.

A. X Force

Substituting the expression for the instantaneous x-body force from Table 1 into Equation 24 produces

$$\begin{aligned}
\overline{X}^B_{RW} = \frac{\omega_{RW}}{2\pi} \Bigg[& \int_0^{\frac{\pi}{\omega_{RW}-\delta_{RW}}} L_{u_{RW}}(t)dt + \int_{\frac{\pi}{\omega_{RW}-\delta_{RW}}}^{\frac{\pi(3\omega_{RW}-2\delta_{RW})}{2\omega_{RW}(\omega_{RW}-\delta_{RW})}} L_{d_{RW}}(t)dt \\
& + \int_{\frac{\pi(3\omega_{RW}-2\delta_{RW})}{2\omega_{RW}(\omega_{RW}-\delta_{RW})}}^{\frac{2\pi}{\omega}} L_{d_{RW}}(t) \Bigg]
\end{aligned} \tag{41}$$

Note that the limits of integration in Equation 41 for the last two integrals define which part of the downstroke is under consideration and hence, which $\phi_{d_{RW}}(t)$ from Equation 10 to use. The integral from $\frac{\pi}{\omega_{RW}-\delta_{RW}}$ to $\frac{\pi(3\omega_{RW}-2\delta_{RW})}{2\omega_{RW}(\omega_{RW}-\delta_{RW})}$ is the first half cycle of the downstroke, while the integral from $\frac{\pi(3\omega_{RW}-2\delta_{RW})}{2\omega_{RW}(\omega_{RW}-\delta_{RW})}$ to $\frac{2\pi}{\omega_{RW}}$ is the second half of the downstroke. Substituting Equation 17 into Equation 41 yields

$$\begin{aligned}\overline{X}^B_{RW} = \frac{k_L\omega_{RW}}{2\pi}\Bigg[&\int_0^{\frac{\pi}{\omega_{RW}-\delta_{RW}}} A^2_{RW}(\omega_{RW}-\delta_{RW})^2\sin^2[(\omega_{RW}-\delta_{RW})t]dt \\ &+\int_{\frac{\pi}{\omega_{RW}-\delta_{RW}}}^{\frac{\pi(3\omega_{RW}-2\delta_{RW})}{2\omega_{RW}(\omega_{RW}-\delta_{RW})}} A^2_{RW}(\omega_{RW}+\sigma_{RW})^2\sin^2[(\omega_{RW}+\sigma_{RW})t+\xi_{RW}]dt \\ &+\int_{\frac{\pi(3\omega_{RW}-2\delta_{RW})}{2\omega_{RW}(\omega_{RW}-\delta_{RW})}}^{\frac{2\pi}{\omega_{RW}}} \left(A_{RW}+\Delta A_{RW}\right)^2(\omega_{RW}+\sigma_{RW})^2\sin^2[(\omega_{RW}+\sigma_{RW})t+\xi_{RW}]dt\Bigg]\end{aligned} \tag{42}$$

Noting that the time varying functions under the integral signs are of the form I_1 and I_4 as given by Equations 25 and 34 respectively, Equation 42 can be written as

$$\begin{aligned}\overline{X}^B_{RW} = \frac{k_L\omega_{RW}}{2\pi}\big[&A^2_{RW}(\omega_{RW}-\delta_{RW})^2 I_1 + A^2_{RW}(\omega_{RW}+\sigma_{RW})^2 I_{41} \\ &+k_L\left(A_{RW}+\Delta A_{RW}\right)^2(\omega_{RW}+\sigma_{RW})^2 I_{42}\big]\end{aligned} \tag{43}$$

or simply

$$\overline{X}^B_{RW} = \frac{k_L\omega_{RW}}{4}\left[A^2_{RW}\left(\omega_{RW}-\delta_{RW}\right)+\frac{(\omega_{RW}+\sigma_{RW})}{2}\left\{A^2_{RW}+\left(A_{RW}+\Delta A_{RW}\right)^2\right\}\right] \tag{44}$$

Following a similar procedure for the left wing, it can be shown that

$$\overline{X}^B_{LW} = \frac{k_L\omega_{LW}}{4}\left[A^2_{LW}\left(\omega_{LW}-\delta_{LW}\right)+\frac{(\omega_{LW}+\sigma_{LW})}{2}\left\{A^2_{LW}+\left(A_{LW}+\Delta A_{LW}\right)^2\right\}\right] \tag{45}$$

Note that both $\overline{X}^B_{RW}$ and $\overline{X}^B_{LW}$ are positive quantities. At a hover condition, where the x-body axis is normal to the surface of the earth, the forces produced by both wings act to counter the weight of the vehicle. Also, from Equations 44 and 45, it can be seen that wing bias has a secondary effect on the vertical force produced and only appears in the $\Delta A_{RW}, \Delta A_{LW}$ terms. In practice, it is expected that $\Delta A_{RW} \ll 1$ and $\Delta A_{LW} \ll 1$ and thus minor changes to vertical force will be experienced by a non-zero wing bias. Recall, from Doman,[12] that when no wing bias is used, $\overline{X}^B_{RW} = \frac{k_L\omega_{RW}}{4}\left(2\omega_{RW}-\delta_{RW}+\sigma_{RW}\right)$ and similarly for the left wing. Comparing this previous result with the expression in Equation 44 and

setting $A_{RW} = 1\ rad$ shows that the increase in x-body axis force, that results from the introduction of a wing bias, is given by $\frac{k_L \omega_{RW}(\omega_{RW}+\sigma_{RW})}{8}\{2\Delta A_{RW} + \Delta A_{RW}^2\}$ and similarly for the left wing.

B. Y Force

The cycle-averaged y-body force for each wing is now considered. Substituting the expression for the instantaneous y-body aerodynamic force from Table 1 into Equation 24 produces

$$\overline{Y}_{RW}^{B} = \frac{\omega_{RW}}{2\pi}\left[\int_0^{\frac{\pi}{\omega_{RW}-\delta_{RW}}} -D_{u_{RW}}(t)\sin[\phi_{u_{RW}}(t)]dt \right. \\ \left. + \int_{\frac{\pi}{\omega_{RW}-\delta_{RW}}}^{\frac{\pi(3\omega_{RW}-2\delta_{RW})}{2\omega_{RW}(\omega_{RW}-\delta_{RW})}} D_{d_{RW}}(t)\sin[\phi_{d_{RW}}(t)]dt + \int_{\frac{\pi(3\omega_{RW}-2\delta_{RW})}{2\omega_{RW}(\omega_{RW}-\delta_{RW})}}^{\frac{2\pi}{\omega}} D_{d_{RW}}(t)\sin[\phi_{d_{RW}}(t)]dt\right] \tag{46}$$

Substituting Equations 10 and 17 into Equation 46 yields

$$\begin{aligned}\overline{Y}_{RW}^{B} = {} & \frac{k_D\omega_{RW}}{2\pi}\int_0^{\frac{\pi}{\omega_{RW}-\delta_{RW}}} -A_{RW}^2(\omega_{RW}-\delta_{RW})^2\sin^2[(\omega_{RW}-\delta_{RW})t] \\ & * \sin\left(A_{RW}\cos[(\omega_{RW}-\delta_{RW})t] + \eta_{RW}\right)dt \\ & + \frac{k_D\omega_{RW}}{2\pi}\int_{\frac{\pi}{\omega_{RW}-\delta_{RW}}}^{\frac{\pi(3\omega_{RW}-2\delta_{RW})}{2\omega_{RW}(\omega_{RW}-\delta_{RW})}} A_{RW}^2(\omega_{RW}+\sigma_{RW})^2\sin^2[(\omega_{RW}+\sigma_{RW})t+\xi_{RW}] \\ & * \sin\left(A_{RW}\cos[(\omega_{RW}+\sigma_{RW})t+\xi_{RW}] + \eta_{RW}\right)dt \\ & + \frac{k_D\omega_{RW}}{2\pi}\int_{\frac{\pi(3\omega_{RW}-2\delta_{RW})}{2\omega_{RW}(\omega_{RW}-\delta_{RW})}}^{\frac{2\pi}{\omega}} (A_{RW}+\Delta A_{RW})^2(\omega_{RW}+\sigma_{RW})^2\sin^2[(\omega_{RW}+\sigma_{RW})t+\xi_{RW}] \\ & * \sin\left(\{A_{RW}+\Delta A_{RW}\}\cos[(\omega_{RW}+\sigma_{RW})t+\xi_{RW}] + \eta_{RW}\right)dt\end{aligned} \tag{47}$$

Using Equations 28, 29, 35, 36, and 37, Equation 47 becomes

$$\begin{aligned}\overline{Y}_{RW}^{B} = \frac{k_D\omega_{RW}}{2\pi}\Big[& -A_{RW}^2(\omega_{RW}-\delta_{RW})^2(I_{21}+I_{22}) + A_{RW}^2(\omega_{RW}+\sigma_{RW})^2(I_{51}+I_{52}) \\ & + \{A_{RW}+\Delta A_{RW}\}^2(\omega_{RW}+\sigma_{RW})^2(I_{53}+I_{54})\Big]\end{aligned} \tag{48}$$

Simplifying Equation 48 yields

$$\begin{aligned}\overline{Y}^{B}_{RW} = & \frac{-k_D A_{RW} J_1(A_{RW}) \omega_{RW} \left(\omega_{RW} - \delta_{RW}\right) \sin \eta_{RW}}{2} \\ & + \frac{k_D \omega_{RW} \left(\omega_{RW} + \sigma_{RW}\right)}{4} \left\{A_{RW} \left(J_1(A_{RW}) \sin \eta_{RW} - H_1(A_{RW}) \cos \eta_{RW}\right)\right\} \\ & + \frac{k_D \omega_{RW} \left(\omega_{RW} + \sigma_{RW}\right)}{4} \left(A_{RW} + \Delta A_{RW}\right) \Big[J_1(A_{RW} + \Delta A_{RW}) \sin \eta_{RW} \\ & + H_1(A_{RW} + \Delta A_{RW}) \cos \eta_{RW} \Big]\end{aligned} \tag{49}$$

From Table 1, it can be seen that the left wing side force has the same form of the right wing side force, except for a minus sign. Hence, for the left wing, it can be shown that

$$\begin{aligned}\overline{Y}^{B}_{LW} = & \frac{k_D A_{LW} J_1(A_{LW}) \omega_{LW} \left(\omega_{LW} - \delta_{LW}\right) \sin \eta_{LW}}{2} \\ & - \frac{k_D \omega_{LW} \left(\omega_{LW} + \sigma_{LW}\right)}{4} \left\{A_{LW} \left(J_1(A_{LW}) \sin \eta_{LW} - H_1(A_{LW}) \cos \eta_{LW}\right)\right\} \\ & - \frac{k_D \omega_{LW} \left(\omega_{LW} + \sigma_{LW}\right)}{4} \left(A_{LW} + \Delta A_{LW}\right) \Big[J_1(A_{LW} + \Delta A_{LW}) \sin \eta_{LW} \\ & + H_1(A_{LW} + \Delta A_{LW}) \cos \eta_{LW} \Big]\end{aligned} \tag{50}$$

Note that when the wing bias is zero ($\eta_{RW} = 0, \eta_{LW} = 0$) the amplitude continuity term is also zero ($\Delta A_{RW} = 0, \Delta A_{LW} = 0$) and $\overline{Y}^{B}_{RW}|_{\eta_{RW}=0} = 0, \overline{Y}^{B}_{LW}|_{\eta_{LW}=0} = 0$. Without wing bias, a side force could not be generated even when using split-cycle frequency modulation. Now, the wing bias has added the ability to generate side forces, although for small wing biases, it is expected that only small side forces could be produced.

C. Z Force

The calculation of the cycle-averaged force in the z-body direction follows a similar procedure. Substituting the expression for the instantaneous z-body aerodynamic force from Table 1 into Equation 24 gives

$$\begin{aligned}\overline{Z}^{B}_{RW} = & \frac{\omega_{RW}}{2\pi} \Bigg[\int_0^{\frac{\pi}{\omega_{RW} - \delta_{RW}}} D_{u_{RW}}(t) \cos[\phi_{u_{RW}}(t)] dt \\ & + \int_{\frac{\pi}{\omega_{RW} - \delta_{RW}}}^{\frac{\pi(3\omega_{RW} - 2\delta_{RW})}{2\omega_{RW}(\omega_{RW} - \delta_{RW})}} -D_{d_{RW}}(t) \cos[\phi_{d_{RW}}(t)] dt + \int_{\frac{\pi(3\omega_{RW} - 2\delta_{RW})}{2\omega_{RW}(\omega_{RW} - \delta_{RW})}}^{\frac{2\pi}{\omega}} -D_{d_{RW}}(t) \cos[\phi_{d_{RW}}(t)] dt \Bigg]\end{aligned} \tag{51}$$

Substituting Equations 10 and 17 into Equation 51 yields

$$\begin{aligned}\overline{Z}^{B}_{RW} = \frac{k_D \omega_{RW}}{2\pi} \Bigg[& \int_{0}^{\frac{\pi}{\omega_{RW}-\delta_{RW}}} A^2_{RW}(\omega_{RW}-\delta_{RW})^2 \sin^2[(\omega_{RW}-\delta_{RW})t] \\ & * \cos\left(A_{RW}\cos[(\omega_{RW}-\delta_{RW})t]+\eta_{RW}\right) dt \\ & - \int_{\frac{\pi}{\omega_{RW}-\delta_{RW}}}^{\frac{\pi(3\omega_{RW}-2\delta_{RW})}{2\omega_{RW}(\omega_{RW}-\delta_{RW})}} A^2_{RW}(\omega_{RW}+\sigma_{RW})^2 \sin^2[(\omega_{RW}+\sigma_{RW})t+\xi_{RW}] \\ & * \cos\left(A_{RW}\cos[(\omega_{RW}+\sigma_{RW})t+\xi_{RW}]+\eta_{RW}\right) dt \\ & - \int_{\frac{\pi(3\omega_{RW}-2\delta_{RW})}{2\omega_{RW}(\omega_{RW}-\delta_{RW})}}^{\frac{2\pi}{\omega}} \left(A_{RW}+\Delta A_{RW}\right)^2 (\omega_{RW}+\sigma_{RW})^2 \sin^2[(\omega_{RW}+\sigma_{RW})t+\xi_{RW}] \\ & * \cos\left(\{A_{RW}+\Delta A_{RW}\}\cos[(\omega_{RW}+\sigma_{RW})t+\xi_{RW}]+\eta_{RW}\right) dt \Bigg]\end{aligned} \tag{52}$$

Noting that the terms of the integrand are of the form I_3 and I_6 as given by Equations 30 and 38 respectively, Equation 52 can be written as

$$\begin{aligned}\overline{Z}^{B}_{RW} = \frac{k_D \omega_{RW}}{2\pi} \Big[& A^2_{RW}(\omega_{RW}-\delta_{RW})^2 (I_{31}+I_{32}) - A^2_{RW}(\omega_{RW}+\sigma_{RW})^2 (I_{61}+I_{62}) \\ & - \{A_{RW}+\Delta A_{RW}\}^2 (\omega_{RW}+\sigma_{RW})^2 (I_{63}+I_{64}) \Big]\end{aligned} \tag{53}$$

Simplifying Equation 53 yields

$$\begin{aligned}\overline{Z}^{B}_{RW} = & \frac{k_D A_{RW} J_1(A_{RW}) \omega_{RW} (\omega_{RW}-\delta_{RW}) \cos\eta_{RW}}{2} \\ & - \frac{k_D \omega_{RW} (\omega_{RW}+\sigma_{RW})}{4} \{A_{RW} (J_1(A_{RW})\cos\eta_{RW} + H_1(A_{RW})\sin\eta_{RW})\} \\ & - \frac{k_D \omega_{RW} (\omega_{RW}+\sigma_{RW})}{4} (A_{RW}+\Delta A_{RW}) \Big[J_1(A_{RW}+\Delta A_{RW})\cos\eta_{RW} \\ & - H_1(A_{RW}+\Delta A_{RW})\sin\eta_{RW} \Big]\end{aligned} \tag{54}$$

For the left wing, the cycle-averaged z force becomes

$$\begin{aligned}\overline{Z}^{B}_{LW} = & \frac{k_D A_{LW} J_1(A_{LW}) \omega_{LW} \left(\omega_{LW} - \delta_{LW}\right) \cos \eta_{LW}}{2} \\ & - \frac{k_D \omega_{LW} \left(\omega_{LW} + \sigma_{LW}\right)}{4} \left\{A_{LW} \left(J_1(A_{LW}) \cos \eta_{LW} + H_1(A_{LW}) \sin \eta_{LW}\right)\right\} \\ & - \frac{k_D \omega_{LW} \left(\omega_{LW} + \sigma_{LW}\right)}{4} \left(A_{LW} + \Delta A_{LW}\right) \Big[J_1(A_{LW} + \Delta A_{LW}) \cos \eta_{LW} \\ & - H_1(A_{LW} + \Delta A_{LW}) \sin \eta_{LW} \Big]\end{aligned} \tag{55}$$

The result for the z-body axis is important because it means that non-zero cycle-averaged forces can be generated and used to induce fore and aft linear accelerations by symmetrically varying the split-cycle parameters. It can also be used to generate rolling moments by asymmetrically (right to left) varying the split-cycle parameters.

The results for the cycle-averaged forces can be simplified to those obtained in Doman[12] by setting $\eta_{RW} = \eta_{LW} = 0$ and $A_{RW} = A_{LW} = 1$.

D. Rolling Moment

For the rolling moment, the expression in Equation 24 becomes

$$\begin{aligned}\overline{M}^{B}_{x\,RW} = & \frac{\omega_{RW}}{2\pi} \Bigg[\int_0^{\frac{\pi}{\omega_{RW} - \delta_{RW}}} M_{x u_{RW}}(t) dt + \int_{\frac{\pi}{\omega_{RW} - \delta_{RW}}}^{\frac{\pi(3\omega_{RW} - 2\delta_{RW})}{2\omega_{RW}(\omega_{RW} - \delta_{RW})}} M_{x d_{RW}}(t) dt \\ & + \int_{\frac{\pi(3\omega_{RW} - 2\delta_{RW})}{2\omega_{RW}(\omega_{RW} - \delta_{RW})}}^{\frac{2\pi}{\omega}} M_{x d_{RW}}(t) dt \Bigg]\end{aligned} \tag{56}$$

Substituting Equations 10 and 17 into Equations 20 and 21, Equation 56 becomes

$$
\begin{aligned}
\overline{M_x}^B_{RW} = \frac{\omega_{RW}}{2\pi} \Bigg[& k_D y_{cp}^{WP} (\omega_{RW} - \delta_{RW})^2 A_{RW}^2 \int_0^{\frac{\pi}{\omega_{RW}-\delta_{RW}}} \sin^2[(\omega_{RW} - \delta_{RW})t] dt \\
& + k_D \frac{w}{2} (\omega_{RW} - \delta_{RW})^2 A_{RW}^2 \int_0^{\frac{\pi}{\omega_{RW}-\delta_{RW}}} \cos\left\{A_{RW} \cos\left[(\omega_{RW} - \delta_{RW})t\right] + \eta_{RW}\right\} \\
& * \sin^2[(\omega_{RW} - \delta_{RW})t] dt \\
& + k_D \Delta z_R^B A_{RW}^2 (\omega_{RW} - \delta_{RW})^2 \int_0^{\frac{\pi}{\omega_{RW}-\delta_{RW}}} \sin\left\{A_{RW} \cos\left[(\omega_{RW} - \delta_{RW})t\right] + \eta_{RW}\right\} \\
& * \sin^2[(\omega_{RW} - \delta_{RW})t] dt \\
& - k_D (\omega_{RW} + \sigma_{RW})^2 y_{cp}^{WP} A_{RW}^2 \int_{\frac{\pi}{\omega_{RW}-\delta_{RW}}}^{\frac{\pi(3\omega_{RW}-2\delta_{RW})}{2\omega_{RW}(\omega_{RW}-\delta_{RW})}} \sin^2\left[(\omega_{RW} + \sigma_{RW})t + \xi_{RW}\right] dt \\
& - k_D (\omega_{RW} + \sigma_{RW})^2 \frac{w}{2} A_{RW}^2 \int_{\frac{\pi}{\omega_{RW}-\delta_{RW}}}^{\frac{\pi(3\omega_{RW}-2\delta_{RW})}{2\omega_{RW}(\omega_{RW}-\delta_{RW})}} \sin^2\left[(\omega_{RW} + \sigma_{RW})t + \xi_{RW}\right] \\
& * \cos\left\{A_{RW} \cos\left[(\omega_{RW} + \sigma_{RW})t + \xi_{RW}\right] + \eta_{RW}\right\} dt \\
& - k_D (\omega_{RW} + \sigma_{RW})^2 \Delta z_R^B A_{RW}^2 \int_{\frac{\pi}{\omega_{RW}-\delta_{RW}}}^{\frac{\pi(3\omega_{RW}-2\delta_{RW})}{2\omega_{RW}(\omega_{RW}-\delta_{RW})}} \sin^2\left[(\omega_{RW} + \sigma_{RW})t + \xi_{RW}\right] \\
& * \sin\left\{A_{RW} \cos\left[(\omega_{RW} + \sigma_{RW})t + \xi_{RW}\right] + \eta_{RW}\right\} dt \\
& - k_D (\omega_{RW} + \sigma_{RW})^2 y_{cp}^{WP} \left(A_{RW} + \Delta A_{RW}\right)^2 \int_{\frac{\pi(3\omega_{RW}-2\delta_{RW})}{2\omega_{RW}(\omega_{RW}-\delta_{RW})}}^{\frac{2\pi}{\omega_{RW}}} \sin^2\left[(\omega_{RW} + \sigma_{RW})t + \xi_{RW}\right] dt \\
& - k_D (\omega_{RW} + \sigma_{RW})^2 \frac{w}{2} \left(A_{RW} + \Delta A_{RW}\right)^2 \int_{\frac{\pi(3\omega_{RW}-2\delta_{RW})}{2\omega_{RW}(\omega_{RW}-\delta_{RW})}}^{\frac{2\pi}{\omega_{RW}}} \sin^2\left[(\omega_{RW} + \sigma_{RW})t + \xi_{RW}\right] \\
& * \cos\left\{\left(A_{RW} + \Delta A_{RW}\right) \cos\left[(\omega_{RW} + \sigma_{RW})t + \xi_{RW}\right] + \eta_{RW}\right\} dt \\
& - k_D (\omega_{RW} + \sigma_{RW})^2 \Delta z_R^B \left(A_{RW} + \Delta A_{RW}\right)^2 \int_{\frac{\pi(3\omega_{RW}-2\delta_{RW})}{2\omega_{RW}(\omega_{RW}-\delta_{RW})}}^{\frac{2\pi}{\omega_{RW}}} \sin^2\left[(\omega_{RW} + \sigma_{RW})t + \xi_{RW}\right] \\
& * \sin\left\{\left(A_{RW} + \Delta A_{RW}\right) \cos\left[(\omega_{RW} + \sigma_{RW})t + \xi_{RW}\right] + \eta_{RW}\right\} dt \Bigg]
\end{aligned}
\tag{57}
$$

Note that the integrals are of the form given in Equations 25 - 40; thus, Equation 57 can be written as

$$\begin{aligned}
\overline{M_x}^B_{RW} &= \frac{\omega_{RW} k_D}{2\pi} \left\{ (\omega_{RW} - \delta_{RW})^2 A_{RW}^2 \left[y_{cp}^{WP} I_1 + \Delta z_R^B I_2 + \frac{w}{2} I_3 \right] \right\} \\
&- \frac{\omega_{RW} k_D}{2\pi} \left\{ (\omega_{RW} + \sigma_{RW})^2 A_{RW}^2 \left[y_{cp}^{WP} I_{41} + \Delta z_R^B \left(I_{51} + I_{52} \right) + \frac{w}{2} \left(I_{61} + I_{62} \right) \right] \right\} \\
&- \frac{\omega_{RW} k_D}{2\pi} \left\{ (\omega_{RW} + \sigma_{RW})^2 \left(A_{RW} + \Delta A_{RW} \right)^2 \left[y_{cp}^{WP} I_{42} + \Delta z_R^B \left(I_{53} + I_{54} \right) + \frac{w}{2} \left(I_{63} + I_{64} \right) \right] \right\}
\end{aligned} \tag{58}$$

Substituting the results for the definite integrals and simplifying yields

$$\begin{aligned}
\overline{M_x}^B_{RW} &= \frac{k_D A_{RW} \omega_{RW} \left(\omega_{RW} - \delta_{RW} \right)}{4} \left[y_{cp}^{WP} A_{RW} + J_1(A_{RW}) \left\{ w \cos \eta_{RW} + 2\Delta z_R^B \sin \eta_{RW} \right\} \right] \\
&- \frac{k_D A_{RW} \omega_{RW} \left(\omega_{RW} + \sigma_{RW} \right)}{8} \left[y_{cp}^{WP} A_{RW} + w \left\{ J_1(A_{RW}) \cos \eta_{RW} + H_1(A_{RW}) \sin \eta_{RW} \right\} \right. \\
&\left. + 2\Delta z_R^B \left\{ J_1(A_{RW}) \sin \eta_{RW} - H_1(A_{RW}) \cos \eta_{RW} \right\} \right] \\
&- \frac{k_D \left(A_{RW} + \Delta A_{RW} \right) \omega_{RW} \left(\omega_{RW} + \sigma_{RW} \right)}{8} \left[y_{cp}^{WP} \left(A_{RW} + \Delta A_{RW} \right) \right. \\
&\left. + w \left\{ J_1 \left(A_{RW} + \Delta A_{RW} \right) \cos \eta_{RW} - H_1 \left(A_{RW} + \Delta A_{RW} \right) \sin \eta_{RW} \right\} \right] \\
&- \frac{k_D \left(A_{RW} + \Delta A_{RW} \right) \omega_{RW} \left(\omega_{RW} + \sigma_{RW} \right)}{8} \left[2\Delta z_R^B \left\{ J_1 \left(A_{RW} + \Delta A_{RW} \right) \sin \eta_{RW} \right. \right. \\
&\left. \left. + H_1 \left(A_{RW} + \Delta A_{RW} \right) \cos \eta_{RW} \right\} \right]
\end{aligned} \tag{59}$$

Following a similar procedure for the left wing, it can be shown that

$$\begin{aligned}
\overline{M_{x_{LW}}}^{B} &= -\frac{k_D A_{LW}\omega_{LW}\left(\omega_{LW}-\delta_{LW}\right)}{4}\left[y_{cp}^{WP}A_{LW}+J_1(A_{LW})\left\{w\cos\eta_{LW}+2\Delta z_L^B\sin\eta_{LW}\right\}\right] \\
&+ \frac{k_D A_{LW}\omega_{LW}\left(\omega_{LW}+\sigma_{LW}\right)}{8}\Bigg[y_{cp}^{WP}A_{LW}+w\left\{J_1(A_{LW})\cos\eta_{LW}+H_1(A_{LW})\sin\eta_{LW}\right\} \\
&+ 2\Delta z_L^B\left\{J_1(A_{LW})\sin\eta_{LW}-H_1(A_{LW})\cos\eta_{LW}\right\}\Bigg] \\
&+ \frac{k_D\left(A_{LW}+\Delta A_{LW}\right)\omega_{LW}\left(\omega_{LW}+\sigma_{LW}\right)}{8}\Bigg[y_{cp}^{WP}\left(A_{LW}+\Delta A_{LW}\right) \\
&+ w\left\{J_1\left(A_{LW}+\Delta A_{LW}\right)\cos\eta_{LW}-H_1\left(A_{LW}+\Delta A_{LW}\right)\sin\eta_{LW}\right\}\Bigg] \\
&+ \frac{k_D\left(A_{LW}+\Delta A_{LW}\right)\omega_{LW}\left(\omega_{LW}+\sigma_{LW}\right)}{8}\Bigg[2\Delta z_L^B\left\{J_1\left(A_{LW}+\Delta A_{LW}\right)\sin\eta_{LW}\right. \\
&+ \left.H_1\left(A_{LW}+\Delta A_{LW}\right)\cos\eta_{LW}\right\}\Bigg]
\end{aligned} \tag{60}$$

When the wing bias terms were not included, then split-cycle frequency modulation was necessary to generate non-zero cycle-averaged rolling moments. Note that, in this case, without split-cycle frequency modulation, i.e., $\delta_{RW}=\sigma_{RW}=\delta_{LW}=\sigma_{LW}=0$, it would be possible to generate non-zero cycle-averaged rolling moments on this aircraft with wing bias. Hence, wing bias has effectively added an additional two control parameters (left and right wing bias) capable of generating rolling moments.

E. Pitching Moment

The cycle-averaged aerodynamic moments in the y-body frame (pitching moment) is now calculated. For the pitching moment, the expression in Equation 24 becomes

$$\begin{aligned}
\overline{M_{y_{RW}}}^{B} = \frac{\omega_{RW}}{2\pi}\Bigg[&\int_0^{\frac{\pi}{\omega_{RW}-\delta_{RW}}} M_{y_{u_{RW}}}(t)dt + \int_{\frac{\pi}{\omega_{RW}-\delta_{RW}}}^{\frac{\pi\left(3\omega_{RW}-2\delta_{RW}\right)}{2\omega_{RW}\left(\omega_{RW}-\delta_{RW}\right)}} M_{y_{d_{RW}}}(t)dt \\
&+ \int_{\frac{\pi\left(3\omega_{RW}-2\delta_{RW}\right)}{2\omega_{RW}\left(\omega_{RW}-\delta_{RW}\right)}}^{\frac{2\pi}{\omega}} M_{y_{d_{RW}}}(t)dt\Bigg]
\end{aligned} \tag{61}$$

Let $C_1 = (\omega_{RW} - \delta_{RW})t$ and $C_2 = (\omega_{RW} + \sigma_{RW})\,t + \xi_{RW}$. Then, substituting Equations 10 and 17 into Equation 61, while using Equations 20 and 21 yields

$$
\begin{aligned}
\overline{M}^{B}_{y_{RW}} = \frac{\omega_{RW}}{2\pi} A^2_{RW}(\omega_{RW} - \delta_{RW})^2 \Bigg\{ & k_L \Delta z^B_R \int_0^{\frac{\pi}{\omega_{RW}-\delta_{RW}}} \sin^2 C_1 dt \\
& - k_D \Delta x^B_R \int_0^{\frac{\pi}{\omega_{RW}-\delta_{RW}}} \sin^2 C_1 \cos\left(A_{RW}\cos C_1 + \eta_{RW}\right) dt \\
& - k_D x^{WP}_{cp} \sin\alpha \int_0^{\frac{\pi}{\omega_{RW}-\delta_{RW}}} \sin^2 C_1 \cos\left(A_{RW}\cos C_1 + \eta_{RW}\right) dt \\
& - k_L x^{WP}_{cp} \cos\alpha \int_0^{\frac{\pi}{\omega_{RW}-\delta_{RW}}} \sin^2 C_1 \cos\left(A_{RW}\cos C_1 + \eta_{RW}\right) dt \\
& + k_L y^{WP}_{cp} \int_0^{\frac{\pi}{\omega_{RW}-\delta_{RW}}} \sin^2 C_1 \sin\left(A_{RW}\cos C_1 + \eta_{RW}\right) dt \Bigg\} \\
& + \frac{\omega_{RW}}{2\pi} A^2_{RW}(\omega_{RW} + \sigma_{RW})^2 \Bigg\{ k_L \Delta z^B_R \int_{\frac{\pi}{\omega_{RW}-\delta_{RW}}}^{\frac{\pi(3\omega_{RW}-2\delta_{RW})}{2\omega_{RW}(\omega_{RW}-\delta_{RW})}} \sin^2 C_2 dt \\
& + k_D \Delta x^B_R \int_{\frac{\pi}{\omega_{RW}-\delta_{RW}}}^{\frac{\pi(3\omega_{RW}-2\delta_{RW})}{2\omega_{RW}(\omega_{RW}-\delta_{RW})}} \sin^2 C_2 \cos\left(A_{RW}\cos C_2 + \eta_{RW}\right) dt \\
& + k_L x^{WP}_{cp} \cos\alpha \int_{\frac{\pi}{\omega_{RW}-\delta_{RW}}}^{\frac{\pi(3\omega_{RW}-2\delta_{RW})}{2\omega_{RW}(\omega_{RW}-\delta_{RW})}} \sin^2 C_2 \cos\left(A_{RW}\cos C_2 + \eta_{RW}\right) dt \\
& + k_D x^{WP}_{cp} \sin\alpha \int_{\frac{\pi}{\omega_{RW}-\delta_{RW}}}^{\frac{\pi(3\omega_{RW}-2\delta_{RW})}{2\omega_{RW}(\omega_{RW}-\delta_{RW})}} \sin^2 C_2 \cos\left(A_{RW}\cos C_2 + \eta_{RW}\right) dt \\
& + k_L y^{WP}_{cp} \int_{\frac{\pi}{\omega_{RW}-\delta_{RW}}}^{\frac{\pi(3\omega_{RW}-2\delta_{RW})}{2\omega_{RW}(\omega_{RW}-\delta_{RW})}} \sin^2 C_2 \sin\left(A_{RW}\cos C_2 + \eta_{RW}\right) dt \Bigg\} \\
& + \frac{\omega_{RW}}{2\pi} \left(A_{RW} + \Delta A_{RW}\right)^2 (\omega_{RW} + \sigma_{RW})^2 \Bigg\{ k_L \Delta z^B_R \int_{\frac{\pi(3\omega_{RW}-2\delta_{RW})}{2\omega_{RW}(\omega_{RW}-\delta_{RW})}}^{\frac{2\pi}{\omega_{RW}}} \sin^2 C_2 dt \\
& + k_D \Delta x^B_R \int_{\frac{\pi(3\omega_{RW}-2\delta_{RW})}{2\omega_{RW}(\omega_{RW}-\delta_{RW})}}^{\frac{2\pi}{\omega_{RW}}} \sin^2 C_2 \cos\left(\left(A_{RW} + \Delta A_{RW}\right)\cos C_2 + \eta_{RW}\right) dt \\
& + k_L x^{WP}_{cp} \cos\alpha \int_{\frac{\pi(3\omega_{RW}-2\delta_{RW})}{2\omega_{RW}(\omega_{RW}-\delta_{RW})}}^{\frac{2\pi}{\omega_{RW}}} \sin^2 C_2 \cos\left(\left(A_{RW} + \Delta A_{RW}\right)\cos C_2 + \eta_{RW}\right) dt \\
& + k_D x^{WP}_{cp} \sin\alpha \int_{\frac{\pi(3\omega_{RW}-2\delta_{RW})}{2\omega_{RW}(\omega_{RW}-\delta_{RW})}}^{\frac{2\pi}{\omega_{RW}}} \sin^2 C_2 \cos\left(\left(A_{RW} + \Delta A_{RW}\right)\cos C_2 + \eta_{RW}\right) dt \\
& + k_L y^{WP}_{cp} \int_{\frac{\pi(3\omega_{RW}-2\delta_{RW})}{2\omega_{RW}(\omega_{RW}-\delta_{RW})}}^{\frac{2\pi}{\omega_{RW}}} \sin^2 C_2 \sin\left(\left(A_{RW} + \Delta A_{RW}\right)\cos C_2 + \eta_{RW}\right) dt \Bigg\}
\end{aligned}
\tag{62}
$$

Note that the integrals are of the form given in Equations 25 - 40; thus, Equation 62 can be written as

$$\begin{aligned}
\overline{M}^{B}_{y_{RW}} =& \frac{\omega_{RW}}{2\pi}\Bigg\{ A^2_{RW}(\omega_{RW}-\delta_{RW})^2\Big[k_L\Delta z^B_R I_1 - k_D\Delta x^B_R I_3 - k_L x^{WP}_{cp}\cos\alpha I_3 \\
&- k_D x^{WP}_{cp}\sin\alpha I_3 + k_L y^{WP}_{cp} I_2\Big] + A^2_{RW}(\omega_{RW}+\sigma_{RW})^2\Big[k_L\Delta z^B_R I_{41} \\
&+ k_D\Delta x^B_R\left(I_{61}+I_{62}\right) + k_L x^{WP}_{cp}\cos\alpha\left(I_{61}+I_{62}\right) \\
&+ k_D x^{WP}_{cp}\sin\alpha\left(I_{61}+I_{62}\right) + k_L y^{WP}_{cp}\left(I_{51}+I_{52}\right)\Big] \\
&+ \left(A_{RW}+\Delta A_{RW}\right)^2\left(\omega_{RW}+\sigma_{RW}\right)^2\Big[k_L\Delta z^B_R I_{42} \\
&+ k_D\Delta x^B_R\left(I_{63}+I_{64}\right) + k_L x^{WP}_{cp}\cos\alpha\left(I_{63}+I_{64}\right) \\
&+ k_D x^{WP}_{cp}\sin\alpha\left(I_{63}+I_{64}\right) + k_L y^{WP}_{cp}\left(I_{53}+I_{54}\right)\Big]\Bigg\}
\end{aligned} \tag{63}$$

Substituting the results for the definite integrals, I_1 - I_6, and simplifying produces

$$\begin{aligned}
\overline{M}^{B}_{y_{RW}} =& \frac{-A_{RW}\omega_{RW}\left(\omega_{RW}-\delta_{RW}\right)}{2}\Bigg[\left(\cos\alpha x^{WP}_{cp}k_L + \left\{\sin\alpha x^{WP}_{cp}+\Delta x^B_R\right\}k_D\right)J_1(A_{RW})\cos\eta_{RW} \\
&- y^{WP}_{cp}k_L J_1(A_{RW})\sin\eta_{RW} - \frac{\Delta z^B_R k_L A_{RW}}{2}\Bigg] \\
&+ \frac{\omega_{RW}\left(\omega_{RW}+\sigma_{RW}\right)}{4A_{RW}}\left(\cos\alpha x^{WP}_{cp}k_L + \left\{\sin\alpha x^{WP}_{cp}+\Delta x^B_R\right\}k_D\right)\Big[A^2_{RW}\left\{J_1(A_{RW})\cos\eta_{RW}\right. \\
&\left. + H_1(A_{RW})\sin\eta_{RW}\right\} + A_{RW}\left(A_{RW}+\Delta A_{RW}\right) \\
&* \left\{J_1\left(A_{RW}+\Delta A_{RW}\right)\cos\eta_{RW} - H_1\left(A_{RW}+\Delta A_{RW}\right)\sin\eta_{RW}\right\}\Big] \\
&+ y^{WP}_{cp}k_L\frac{\omega_{RW}\left(\omega_{RW}+\sigma_{RW}\right)}{4A_{RW}}\Big[A^2_{RW}\left\{J_1(A_{RW})\sin\eta_{RW} - H_1(A_{RW})\cos\eta_{RW}\right\} \\
&+A_{RW}\left(A_{RW}+\Delta A_{RW}\right)\left\{J_1\left(A_{RW}+\Delta A_{RW}\right)\sin\eta_{RW} + H_1\left(A_{RW}+\Delta A_{RW}\right)\cos\eta_{RW}\right\}\Big] \\
&+ \frac{\Delta z^B_R k_L\omega_{RW}\left(\omega_{RW}+\sigma_{RW}\right)}{8}\left[A^2_{RW} + \left(A_{RW}+\Delta A_{RW}\right)^2\right]
\end{aligned} \tag{64}$$

Following a similar procedure for the left wing, it can be shown that

$$\begin{aligned}
\overline{M_y}^B_{LW} = & \frac{-A_{LW}\omega_{LW}\left(\omega_{LW}-\delta_{LW}\right)}{2}\Bigg[\left(\cos\alpha x_{cp}^{WP}k_L+\left\{\sin\alpha x_{cp}^{WP}+\Delta x_L^B\right\}k_D\right)J_1(A_{LW})\cos\eta_{LW} \\
& - y_{cp}^{WP}k_L J_1(A_{LW})\sin\eta_{LW}-\frac{\Delta z_L^B k_L A_{LW}}{2}\Bigg] \\
& + \frac{\omega_{LW}\left(\omega_{LW}+\sigma_{LW}\right)}{4A_{LW}}\left(\cos\alpha x_{cp}^{WP}k_L+\left\{\sin\alpha x_{cp}^{WP}+\Delta x_L^B\right\}k_D\right)\Bigg[A_{LW}^2\left\{J_1(A_{LW})\cos\eta_{LW}\right. \\
& \left. + H_1(A_{LW})\sin\eta_{LW}\right\}+A_{LW}\left(A_{LW}+\Delta A_{LW}\right) \\
& * \left\{J_1\left(A_{LW}+\Delta A_{LW}\right)\cos\eta_{LW}-H_1\left(A_{LW}+\Delta A_{LW}\right)\sin\eta_{LW}\right\}\Bigg] \\
& + y_{cp}^{WP}k_L\frac{\omega_{LW}\left(\omega_{LW}+\sigma_{LW}\right)}{4A_{LW}}\Bigg[A_{LW}^2\left\{J_1(A_{LW})\sin\eta_{LW}-H_1(A_{LW})\cos\eta_{LW}\right\} \\
& + A_{LW}\left(A_{LW}+\Delta A_{LW}\right)\left\{J_1\left(A_{LW}+\Delta A_{LW}\right)\sin\eta_{LW}+H_1\left(A_{LW}+\Delta A_{LW}\right)\cos\eta_{LW}\right\}\Bigg] \\
& + \frac{\Delta z_L^B k_L\omega_{LW}\left(\omega_{LW}+\sigma_{LW}\right)}{8}\left[A_{LW}^2+\left(A_{LW}+\Delta A_{LW}\right)^2\right]
\end{aligned} \tag{65}$$

Note that without split-cycle frequency modulation, i.e., $\delta_{RW}=\sigma_{RW}=\delta_{LW}=\sigma_{LW}=0$, there still exists a non-zero cycle-averaged pitching moment if $\Delta z_R^B\neq 0$ and $\Delta z_L^B\neq 0$. Setting $\Delta z_R^B=0, \Delta z_L^B=0$ will yield a zero cycle-averaged pitching moment when the split-cycle parameters and wing biases are zero, which is a desirable feature for maintaining hover. Also note that the wing bias appears throughout these expressions and thus will have an impact on the pitching moment of the vehicle. To obtain a more quantitative estimate of cycle-averaged pitching moment change due to wing bias, Equation 64 can be rewritten with $\Delta z_R^B=0$, $\sin\eta_{RW}=0$, $\cos\eta_{RW}=1$, $A_{RW}=1\ rad$, and $\left(\cos\alpha x_{cp}^{WP}k_L+\left\{\sin\alpha x_{cp}^{WP}+\Delta x_R^B\right\}k_D\right)=M$ to obtain

$$\begin{aligned}
\overline{M_y}^B_{RW} = & \frac{-\omega_{RW}\left(\omega_{RW}-\delta_{RW}\right)}{2}MJ_1(1) \\
& + \frac{\omega_{RW}\left(\omega_{RW}+\sigma_{RW}\right)}{4}M\left[J_1(1)+\left(1+\Delta A_{RW}\right)J_1\left(1+\Delta A_{RW}\right)\right] \\
& + y_{cp}^{WP}k_L\frac{\omega_{RW}\left(\omega_{RW}+\sigma_{RW}\right)}{4}\left[-H_1(1)+\left(1+\Delta A_{RW}\right)H_1\left(1+\Delta A_{RW}\right)\right]
\end{aligned} \tag{66}$$

When $\Delta A=0$, $J_1(1)+\left(1+\Delta A_{RW}\right)J_1\left(1+\Delta A_{RW}\right)=2J_1(1)=.8801$ and $-H_1(1)+\left(1+\Delta A_{RW}\right)H_1\left(1+\Delta A_{RW}\right)=0$. For $\Delta A=0.2\ rad$, $J_1(1)+\left(1+\Delta A_{RW}\right)J_1\left(1+\Delta A_{RW}\right)=J_1(1)+1.2J_1(1.2)=1.038$ and $-H_1(1)+(1+0.2)H_1(1.2)=0.1344$. Thus, a change in the second and third terms in Equation 66 on the order of 15% can be expected; therefore, even a small wing bias can significantly alter the cycle-averaged pitching moment. Figure 4 shows $H_1(A)$ and $J_1(A)$ vs. A. The slopes of the Bessel function of the first kind and the Struve function about $A=1$ are nearly the same, thus it is expected that both the second and third terms in Equation 66 will impact the cycle-averaged pitching moment. In other words, when computing the change in pitching

moment due to a change in η, the chain rule is used to obtain $\frac{\partial J_1(1+\Delta A_{RW})}{\partial \eta_{RW}} = \frac{\partial J_1(1+\Delta A_{RW})}{\partial \Delta A_{RW}} \frac{\partial \Delta A_{RW}}{\partial \eta_{RW}}$ and $\frac{\partial H_1(1+\Delta A_{RW})}{\partial \eta_{RW}} = \frac{\partial H_1(1+\Delta A_{RW})}{\partial \Delta A_{RW}} \frac{\partial \Delta A_{RW}}{\partial \eta_{RW}}$. Since the derivatives of the Bessel function of the first kind and the Struve function with respect to A are non-zero about $A = 1$, the second and third terms in Equation 66 will create pitching moment increments.

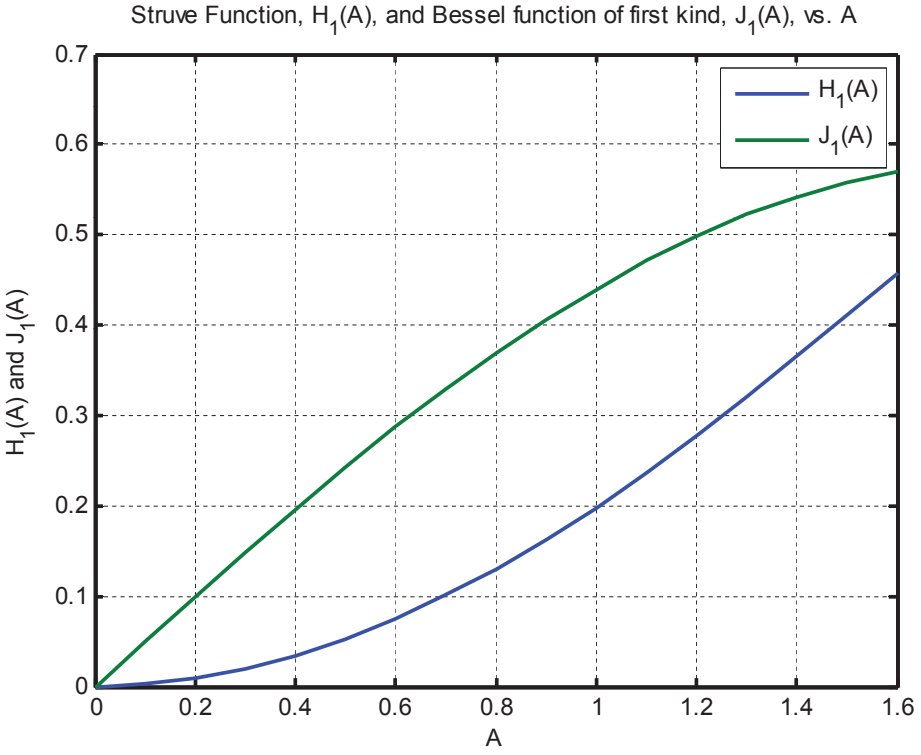

Figure 4. $H_1(A)$ **and** $J_1(A)$ **vs.** A**.**

F. Yawing Moment

The cycle-averaged yawing moment (z-body moment) is calculated in the same fashion. Substituting the expression for the instantaneous z-body moment from Equations 20 and 21 into Equation 24 produces

$$\overline{M_z}^B_{RW} = \frac{\omega_{RW}}{2\pi} \left[\int_0^{\frac{\pi}{\omega_{RW}-\delta_{RW}}} M_{z_{u_{RW}}}(t)dt + \int_{\frac{\pi}{\omega_{RW}-\delta_{RW}}}^{\frac{\pi(3\omega_{RW}-2\delta_{RW})}{2\omega_{RW}(\omega_{RW}-\delta_{RW})}} M_{z_{d_{RW}}}(t)dt + \int_{\frac{\pi(3\omega_{RW}-2\delta_{RW})}{2\omega_{RW}(\omega_{RW}-\delta_{RW})}}^{\frac{2\pi}{\omega_{RW}}} M_{z_{d_{RW}}}(t)dt \right] \tag{67}$$

Again, let $C_1 = (\omega_{RW} - \delta_{RW})t$ and $C_2 = (\omega_{RW} + \sigma_{RW})\,t + \xi_{RW}$. Substituting Equations 10 and 17 into Equation 67, while using Equations 10 and 17, yields

$$
\begin{aligned}
\overline{M}^{B}_{z\,RW} = \frac{\omega_{RW}}{2\pi} \Bigg\{ & A^2_{RW}(\omega_{RW} - \delta_{RW})^2 \Bigg[-k_L \frac{w}{2} \int_0^{\frac{\pi}{\omega_{RW} - \delta_{RW}}} \sin^2 C_1 dt \\
& - k_D \Delta x^B_R \int_0^{\frac{\pi}{\omega_{RW} - \delta_{RW}}} \sin^2 C_1 \sin\{A_{RW} \cos C_1 + \eta_{RW}\}\, dt \\
& - k_L y^{WP}_{cp} \int_0^{\frac{\pi}{\omega_{RW} - \delta_{RW}}} \sin^2 C_1 \cos\{A_{RW} \cos C_1 + \eta_{RW}\}\, dt \\
& - k_L x^{WP}_{cp} \cos\alpha \int_0^{\frac{\pi}{\omega_{RW} - \delta_{RW}}} \sin^2[(\omega_{RW} - \delta_{RW})t] \sin\{A_{RW} \cos C_1 + \eta_{RW}\}\, dt \\
& - k_D x^{WP}_{cp} \sin\alpha \int_0^{\frac{\pi}{\omega_{RW} - \delta_{RW}}} \sin^2[(\omega_{RW} - \delta_{RW})t] \sin\{A_{RW} \cos C_1 + \eta_{RW}\}\, dt \Bigg] \\
& + A^2_{RW}(\omega_{RW} + \sigma_{RW})^2 \Bigg[-k_L \frac{w}{2} \int_{\frac{\pi}{\omega_{RW} - \delta_{RW}}}^{\frac{\pi(3\omega_{RW} - 2\delta_{RW})}{2\omega_{RW}(\omega_{RW} - \delta_{RW})}} \sin^2 C_2 dt \\
& + k_D \Delta x^B_R \int_{\frac{\pi}{\omega_{RW} - \delta_{RW}}}^{\frac{\pi(3\omega_{RW} - 2\delta_{RW})}{2\omega_{RW}(\omega_{RW} - \delta_{RW})}} \sin^2 C_2 \sin\{A_{RW} \cos C_2 + \eta_{RW}\}\, dt \\
& - k_L y^{WP}_{cp} \int_{\frac{\pi}{\omega_{RW} - \delta_{RW}}}^{\frac{\pi(3\omega_{RW} - 2\delta_{RW})}{2\omega_{RW}(\omega_{RW} - \delta_{RW})}} \sin^2 C_2 \cos\{A_{RW} \cos C_2 + \eta_{RW}\}\, dt \\
& + k_L x^{WP}_{cp} \cos\alpha \int_{\frac{\pi}{\omega_{RW} - \delta_{RW}}}^{\frac{\pi(3\omega_{RW} - 2\delta_{RW})}{2\omega_{RW}(\omega_{RW} - \delta_{RW})}} \sin^2 C_2 \sin\{A_{RW} \cos C_2 + \eta_{RW}\}\, dt \\
& + k_D x^{WP}_{cp} \sin\alpha \int_{\frac{\pi}{\omega_{RW} - \delta_{RW}}}^{\frac{\pi(3\omega_{RW} - 2\delta_{RW})}{2\omega_{RW}(\omega_{RW} - \delta_{RW})}} \sin^2 C_2 \sin\{A_{RW} \cos C_2 + \eta_{RW}\}\, dt \Bigg] \\
& + (A_{RW} + \Delta A_{RW})^2 (\omega_{RW} + \sigma_{RW})^2 \Bigg[-k_L \frac{w}{2} \int_{\frac{\pi(3\omega_{RW} - 2\delta_{RW})}{2\omega_{RW}(\omega_{RW} - \delta_{RW})}}^{\frac{2\pi}{\omega_{RW}}} \sin^2 C_2 dt \\
& + k_D \Delta x^B_R \int_{\frac{\pi(3\omega_{RW} - 2\delta_{RW})}{2\omega_{RW}(\omega_{RW} - \delta_{RW})}}^{\frac{2\pi}{\omega_{RW}}} \sin^2 C_2 \sin\{(A_{RW} + \Delta A_{RW}) \cos C_2 + \eta_{RW}\}\, dt \\
& - k_L y^{WP}_{cp} \int_{\frac{\pi(3\omega_{RW} - 2\delta_{RW})}{2\omega_{RW}(\omega_{RW} - \delta_{RW})}}^{\frac{2\pi}{\omega_{RW}}} \sin^2 C_2 \cos\{(A_{RW} + \Delta A_{RW}) \cos C_2 + \eta_{RW}\}\, dt \\
& + k_L x^{WP}_{cp} \cos\alpha \int_{\frac{\pi(3\omega_{RW} - 2\delta_{RW})}{2\omega_{RW}(\omega_{RW} - \delta_{RW})}}^{\frac{2\pi}{\omega_{RW}}} \sin^2 C_2 \sin\{(A_{RW} + \Delta A_{RW}) \cos C_2 + \eta_{RW}\}\, dt \\
& + k_D x^{WP}_{cp} \sin\alpha \int_{\frac{\pi(3\omega_{RW} - 2\delta_{RW})}{2\omega_{RW}(\omega_{RW} - \delta_{RW})}}^{\frac{2\pi}{\omega_{RW}}} \sin^2 C_2 \sin\{(A_{RW} + \Delta A_{RW}) \cos C_2 + \eta_{RW}\}\, dt \Bigg] \Bigg\}
\end{aligned}
\tag{68}
$$

Note that the integrals are of the form given in Equations 25-40; thus, Equation 68 can be written as

$$\begin{aligned}
\overline{M}^{B}_{z\,RW} =& \frac{\omega_{RW}}{2\pi}\Bigg\{A^2_{RW}(\omega_{RW}-\delta_{RW})^2\Bigg[-k_L\frac{w}{2}I_1-k_D\Delta x^B_R I_2-k_L y^{WP}_{cp}I_3 \\
&-k_L x^{WP}_{cp}\cos\alpha I_2-k_D x^{WP}_{cp}\sin\alpha I_2\Bigg]+A^2_{RW}(\omega_{RW}+\sigma_{RW})^2\Bigg[-k_L\frac{w}{2}I_{41} \\
&+k_D\Delta x^B_R\left(I_{51}+I_{52}\right)-k_L y^{WP}_{cp}\left(I_{61}+I_{62}\right) \\
&+k_L x^{WP}_{cp}\cos\alpha\left(I_{51}+I_{52}\right)+k_D x^{WP}_{cp}\sin\alpha\left(I_{51}+I_{52}\right)\Bigg] \\
&+\left(A_{RW}+\Delta A_{RW}\right)^2\left(\omega_{RW}+\sigma_{RW}\right)^2\Bigg[-k_L\frac{w}{2}I_{42}+k_D\Delta x^B_R\left(I_{53}+I_{54}\right) \\
&-k_L y^{WP}_{cp}\left(I_{63}+I_{64}\right)+k_L x^{WP}_{cp}\cos\alpha\left(I_{53}+I_{54}\right)+k_D x^{WP}_{cp}\sin\alpha\left(I_{53}+I_{54}\right)\Bigg]\Bigg\}
\end{aligned} \tag{69}$$

Substituting the results for the definite integrals, I_1-I_6, and simplifying gives

$$\begin{aligned}
\overline{M}^{B}_{z\,RW} =& \frac{A_{RW}\omega_{RW}\left(\omega_{RW}-\delta_{RW}\right)}{2}\Bigg[J_1(A_{RW})\sin\eta_{RW}\Big\{-k_D\left(\sin\alpha x^{WP}_{cp}+\Delta x^B_R\right) \\
&-\cos\alpha x^{WP}_{cp}k_L-y^{WP}_{cp}k_L\frac{\cos\eta_{RW}}{\sin\eta_{RW}}\Big\}-\frac{wk_LA_{RW}}{4}\Bigg] \\
&+\frac{k_DA_{RW}\omega_{RW}\left(\omega_{RW}+\sigma_{RW}\right)}{4}\left(\sin\alpha x^{WP}_{cp}+\Delta x^B_R\right)\Bigg(J_1(A_{RW})\sin\eta_{RW} \\
&-H_1(A_{RW})\cos\eta_{RW}\Bigg) \\
&-\frac{k_LA_{RW}\omega_{RW}\left(\omega_{RW}+\sigma_{RW}\right)}{4}\Bigg(-\cos\alpha x^{WP}_{cp}\Big\{J_1(A_{RW})\sin\eta_{RW} \\
&-H_1(A_{RW})\cos\eta_{RW}\}+y^{WP}_{cp}\{J_1(A_{RW})\cos\eta_{RW}+H_1(A_{RW})\sin\eta_{RW}\Big\}+\frac{wA_{RW}}{4}\Bigg) \\
&+\frac{k_D\left(A_{RW}+\Delta A_{RW}\right)\omega_{RW}\left(\omega_{RW}+\sigma_{RW}\right)}{4}\left(\sin\alpha x^{WP}_{cp}+\Delta x^B_R\right) \\
&*\left(J_1(A_{RW}+\Delta A_{RW})\sin\eta_{RW}+H_1(A_{RW}+\Delta A_{RW})\cos\eta_{RW}\right) \\
&-\frac{k_L\left(A_{RW}+\Delta A_{RW}\right)\omega_{RW}\left(\omega_{RW}+\sigma_{RW}\right)}{4}\Bigg(-\cos\alpha x^{WP}_{cp} \\
&*\left\{J_1(A_{RW}+\Delta A_{RW})\sin\eta_{RW}+H_1(A_{RW}+\Delta A_{RW})\cos\eta_{RW}\right\} \\
&+y^{WP}_{cp}\left\{J_1(A_{RW}+\Delta A_{RW})\cos\eta_{RW}-H_1(A_{RW}+\Delta A_{RW})\sin\eta_{RW}\right\} \\
&+\frac{w\left(A_{RW}+\Delta A_{RW}\right)}{4}\Bigg)
\end{aligned} \tag{70}$$

Following a similar procedure for the left wing, it can be shown that

$$
\begin{aligned}
\overline{M_z}^B_{LW} = & -\frac{A_{LW}\omega_{LW}\left(\omega_{LW}-\delta_{LW}\right)}{2}\left[J_1(A_{LW})\sin\eta_{LW}\left\{-k_D\left(\sin\alpha x_{cp}^{WP}+\Delta x_L^B\right)\right.\right. \\
& \left.\left.-\cos\alpha x_{cp}^{WP}k_L - y_{cp}^{WP}k_L\frac{\cos\eta_{LW}}{\sin\eta_{LW}}\right\} - \frac{wk_LA_{LW}}{4}\right] \\
& -\frac{k_DA_{LW}\omega_{LW}\left(\omega_{LW}+\sigma_{LW}\right)}{4}\left(\sin\alpha x_{cp}^{WP}+\Delta x_L^B\right)\left(J_1(A_{LW})\sin\eta_{LW}\right. \\
& \left.-H_1(A_{LW})\cos\eta_{LW}\right) \\
& +\frac{k_LA_{LW}\omega_{LW}\left(\omega_{LW}+\sigma_{LW}\right)}{4}\left(-\cos\alpha x_{cp}^{WP}\left\{J_1(A_{LW})\sin\eta_{LW}\right.\right. \\
& \left.\left.-H_1(A_{LW})\cos\eta_{LW}\right\}+y_{cp}^{WP}\left\{J_1(A_{LW})\cos\eta_{LW}+H_1(A_{LW})\sin\eta_{LW}\right\}+\frac{wA_{LW}}{4}\right) \\
& -\frac{k_D\left(A_{LW}+\Delta A_{LW}\right)\omega_{LW}\left(\omega_{LW}+\sigma_{LW}\right)}{4}\left(\sin\alpha x_{cp}^{WP}+\Delta x_L^B\right) \\
& *\left(J_1(A_{LW}+\Delta A_{LW})\sin\eta_{LW}+H_1(A_{LW}+\Delta A_{LW})\cos\eta_{LW}\right) \\
& +\frac{k_L\left(A_{LW}+\Delta A_{LW}\right)\omega_{LW}\left(\omega_{LW}+\sigma_{LW}\right)}{4}\left(-\cos\alpha x_{cp}^{WP}\right. \\
& *\left\{J_1(A_{LW}+\Delta A_{LW})\sin\eta_{LW}+H_1(A_{LW}+\Delta A_{LW})\cos\eta_{LW}\right\} \\
& +y_{cp}^{WP}\left\{J_1(A_{LW}+\Delta A_{LW})\cos\eta_{LW}-H_1(A_{LW}+\Delta A_{LW})\sin\eta_{LW}\right\} \\
& \left.+\frac{w\left(A_{LW}+\Delta A_{LW}\right)}{4}\right)
\end{aligned}
\tag{71}
$$

Note that without split-cycle frequency modulation, there exists a non-zero cycle-averaged yawing moment on each wing since $y_{cp}^{WP} \neq 0$ and $w \neq 0$. When the split-cycle parameters for each wing are zero and $\omega_{RW} = \omega_{LW}$, the cycle-averaged moments are opposing and balance one another. Since the fundamental wingbeat frequency, ω, can be independently varied for each wing, yawing moments can be generated without varying the split-cycle parameters or wing bias terms. Nevertheless, the bias terms are also present in Equations 70 and 71 and therefore can be used to generate yawing moments. This is because there is a difference in the moment arm from left to right.

VI. Conclusions

The analysis presented shows that the use of split-cycle constant-period frequency modulation with wing bias and independently actuated wings allows one to manipulate the x-body and z-body axis forces. The y-body force is also controllable using this approach, however, since small wing bias terms are needed to perform typical maneuvers, the available cycle-averaged y-body axis

forces are small. Rolling, pitching, and yawing moments can also be generated using the split-cycle technique with wing bias and it appears that wing bias can significantly change the cycle-averaged pitching moment. Given the ability to manipulate the cycle-averaged body-axis forces and moments, untethered controlled flight with insect-like maneuverability appears to be feasible with only two physical actuators, which is supported by the simulation results presented in Part II.[34]

References

[1]Osborne, M. F. M., "Aerodynamics of flapping flight with application to insects," *Journal of Experimental Biology*, Vol. 28, 1951, pp. 221–245.

[2]Jensen, M., "Biology and physics of locust flight III. The aerodynamics of locust flight," *Philosophical Transactions of the Royal Society of London: Series B: Biological Series*, Vol. 239, 1956.

[3]Vogel, S., "Flight in Drosophila II. Variations in stroke parameters and wing contour," *Journal of Experimental Biology*, Vol. 46, 1967, pp. 383–392.

[4]Vogel, S., "Flight in Drosophila III. Aerodynamic characteristics of fly wings and wing models," *Journal of Experimental Biology*, Vol. 46, 1967, pp. 431–443.

[5]Sane, S. P. and Dickenson, M. H., "The Control of Flight Force by a Flapping Wing: Lift and Drag Force Production," *The Journal of Experimental Biology*, Vol. 204, 2001, pp. 2607–2626.

[6]Sane, S. P. and Dickenson, M. H., "The aerodynamic effects of wing rotation and a revised quasi-steady model of flapping flight," *The Journal of Experimental Biology*, Vol. 205, 2002, pp. 1087–1096.

[7]Wood, R. J., "The First Takeoff of a Biologically Inspired At-Scale Robotic Insect," *IEEE Transactions on Robotics*, Vol. 24, No. 2, 2007, pp. 341–347.

[8]Wood, R. J., "Design, fabrication, and analysis of a 3DOF, 3cm flapping-wing MAV," Proceedings of the 2007 IEEE/RSJ International Conference on Intelligent Robots and Systems, Oct. 2007.

[9]Ellington, C. P., "The aerodynamics of hovering insect flight I. The Quasi-Steady analysis," *Philosophical Transactions of the Royal Society of London: Series B: Biological Series*, Vol. 305, 1984.

[10]Dudley, R. and Ellington, C. P., "Mechanics of forward flight in bumblebees I. Kinematics and morphology," *Journal of Experimental Biology*, Vol. 148, 1990, pp. 19–52.

[11]Dudley, R. and Ellington, C. P., "Mechanics of forward flight in bumblebees II. Quasi-Steady lift and power requirements," *Journal of Experimental Biology*, Vol. 148, 1990, pp. 55–88.

[12]Doman, D. B., Oppenheimer, M. W., and Sigthorsson, D. O., "Dynamics and Control of a Minimally Actuated Biomimetic Vehicle: Part I - Aerodynamic Model," *AIAA Guidance, Navigation and Control Conference*, AIAA-2009-6160, Aug. 2009.

[13]Oppenheimer, M. W., Doman, D. B., and Sigthorsson, D. O., "Dynamics and Control of a Minimally Actuated Biomimetic Vehicle: Part II - Control," *AIAA Guidance, Navigation and Control Conference*, AIAA-2009-6161, Aug. 2009.

[14]Ellington, C. P., "The aerodynamics of hovering insect flight II. Morphological parameters," *Philosophical Transactions of the Royal Society of London: Series B: Biological Series*, Vol. 305, 1984.

[15]Ellington, C. P., "The aerodynamics of hovering insect flight III. Kinematics," *Philosophical Transactions of the Royal Society of London: Series B: Biological Series*, Vol. 305, 1984.

[16]Ellington, C. P., "The aerodynamics of hovering insect flight IV. Aerodynamic mechanisms," *Philosophical Transactions of the Royal Society of London: Series B: Biological Series*, Vol. 305, 1984.

[17]Ellington, C. P., "The aerodynamics of hovering insect flight V. A vortex theory," *Philosophical Transactions of the Royal Society of London: Series B: Biological Series*, Vol. 305, 1984.

[18]Ellington, C. P., "The aerodynamics of hovering insect flight VI. Lift and power requirements," *Philosophical Transactions of the Royal Society of London: Series B: Biological Series*, Vol. 305, 1984.

[19]Dudley, R., "Biomechanics of flight in neotropical butterflies: aerodynamics and mechanical power requirements," *Journal of Experimental Biology*, Vol. 159, 1991, pp. 335–357.

[20]Ennos, A. R., "The kinematics and aerodynamics of the free flight of some Diptera," *Journal of Experimental Biology*, Vol. 142, 1989, pp. 49–85.

[21]Willmott, A. P. and Ellington, C. P., "The mechanisms of flight in the hawkmoth Manduca Sexta I. Kinematics of hovering and forward flight," *Journal of Experimental Biology*, Vol. 200, 1997, pp. 2705–2722.

[22]Willmott, A. P. and Ellington, C. P., "The mechanisms of flight in the hawkmoth Manduca Sexta II. Aerodynamic consequences of kinematic and morphological variation," *Journal of Experimental Biology*, Vol. 200, 1997, pp. 2723–2745.

[23]Willmott, A. P., Ellington, C. P., and Thomas, A. L. R., "Flow visualization and unsteady aerodynamics in the flight of the hawkmoth Manduca Sexta," *Philosophical Transactions of the Royal Society of London: Series B: Biological Series*, Vol. 352, 1997.

[24]Shyy, W., Lain, Y., Tang, J., Viieru, D., and Lui, H., *Aerodynamics of low Reynolds number flyers*, Cambridge University Press, New York, NY, 2008.

[25]Deng, X., Schenato, L., Wu, W. C., and Sastry, S. S., "Flapping flight for biomimetic robotic insects: Part I - system modeling," *IEEE Trans. on Robotics*, Vol. 22, No. 4, 2006, pp. 776–788.

[26]*Ż*bikowski, R., "On aerodynamic modelling of an insect-like flapping wing in hover for micro air vehicles," *Philosophical Transactions of the Royal Society of London: Series A*, Vol. 360, 2002.

[27]Sane, S. P., "The aerodynamics of insect flight," *Journal of Experimental Biology*, Vol. 206, 2003, pp. 4191–4208.

[28]Dickinson, M. H. and *Götz*, K. G., "Unsteady aerodynamic performance of model wings at low Reynolds numbers," *Journal of Experimental Biology*, Vol. 174, 1993, pp. 45–64.

[29]Sitaraman, J., Roget, B., Harmon, R., Graurer, J., Conroy, J., Hubbard, J., and Humbert, S., "A computational study of flexible wing ornithopter flight," AIAA-2008-6397.

[30]Deng, X., Schenato, L., Wu, W. C., and Sastry, S. S., "Flapping flight for biomimetic robotic insects: Part II - flight control design," *IEEE Trans. on Robotics*, Vol. 22, No. 4, 2006, pp. 789–803.

[31]Deng, X., Schenato, L., and Sastry, S. S., "Hovering flight control of a micromechanical flying insect," *IEEE Conference on Decision and Control*, IEEE-0-7803-7061-9, Dec. 2001.

[32]Doman, D. B., Oppenheimer, M. W., and Bolender, M. A., "Altitude Control of a Single Degree of Freedom Flapping Wing Micro Air Vehicle," *AIAA Guidance, Navigation and Control Conference*, AIAA-2009-6159, Aug. 2009.

[33]Wood, R.J., Steltz E., and Fearing, R.S. , "Optimal Energy Density Piezoelectric Bending Actuators," *Sensors and Actuators A: Physical*, Vol. 119, 2005, pp. 476–488.

[34]Doman, D. B., Oppenheimer, M. W., and Sigthorsson, D. O., "Dynamics and Control of a Biomimetic Vehicle Using Biased Wingbeat Forcing Functions: Part II - Controller," Submitted to 2010 AIAA Aerosciences Conference, 2010.

[35]Gradshteyn, I.S. and Ryzhik, I.M., *Table of Integrals, Series and Products, 6 ed.*, Academic Press, 2000.